The $^{40}Ar/^{39}Ar$ chronology and eruption rates of Cenozoic volcanism in the eastern Bering Sea Volcanic Province, Alaska

Samuel B. Mukasa,[1] Alexander V. Andronikov,[1] and Chris M. Hall[1]

Received 17 April 2006; revised 2 January 2007; accepted 21 February 2007; published 26 June 2007.

[1] The eastern sector of the Bering Sea Volcanic Province, Alaska, consists of a number of large late Cenozoic volcanic fields that occur in a broad region inboard from the Aleutian arc front to the Arctic Circle. We estimate that about 750 km^3 of magma were erupted in the volcanic centers that we have studied, all within the past 6.0 Ma. Several discrete eruption episodes have been identified with the new $^{40}Ar/^{39}Ar$ data at circa 6.0 Ma (Imuruk volcanic field), circa 3.5 Ma (Teller volcanic field), circa 2.5–1.5 Ma (St. George Island), circa 1.0 Ma (St. Lawrence Island), and the youngest activity which started at circa 0.7 Ma and continued throughout region until historic times. Combining age information with volume estimates reveals that the intensity of volcanic activity in the Bering Sea Volcanic Province has increased through time, with only about 15% of lava erupted before 3 Ma and about 30% of all late Cenozoic magma erupted within the last 500 ka. Eruption rates also increase toward more recent times, from the 6 Ma Imuruk basalts, which erupted at the rate of $\sim 70 \pm 15$ m^3 km^{-2} yr^{-1}, to the ≤ 0.7 Ma Nunivak Island and St. Michael volcanic field basalts, which erupted at a rate of $\sim 165 \pm 25$ m^3 km^{-2} yr^{-1}. High volumes of erupted lava accompanied by high eruption rates for the youngest volcanic rocks suggest significant changes in the melting rates, which are best explained by either an evolving tectonic regime or significant changes in the melting processes.

Citation: Mukasa, S. B., A. V. Andronikov, and C. M. Hall (2007), The $^{40}Ar/^{39}Ar$ chronology and eruption rates of Cenozoic volcanism in the eastern Bering Sea Volcanic Province, Alaska, *J. Geophys. Res.*, *112*, B06207, doi:10.1029/2006JB004452.

1. Introduction

1.1. Tectonic Setting

[2] Northwestern Alaska, the adjacent northern Bering Sea region and northeastern Arctic Russia are situated near the boundary between the Eurasian and North American plates. These areas are composed of variably extended continental lithospheric materials that in a few places are separated by rocks of oceanic affinity [*Patton and Box*, 1989; *Miller and Hudson*, 1991; *Patton et al.*, 1994; *Plafker and Berg*, 1994]. The Lower Paleozoic record of the area is dominated by platform sequences indicative of relatively stable tectonics, though this is punctuated by at least one episode of rifting [*Till and Dumoulin*, 1994, references therein]. In contrast, the Mesozoic history of the area is dominated by convergence, terrane accretion, and plutonism associated with a northward dipping subduction zone active during the amalgamation of terranes comprising modern Alaska [*Plafker and Berg*, 1994; *Amato and Wright*, 1997].

[3] The Bering Sea Volcanic Province (BSVP) (Figure 1) developed over this extended continental lithosphere beginning at ~30 Ma, as an isolated event, with the eruption of the Koyuk-Buckland volcanic field (9 on the map in Figure 1), just northeast of Seward Peninsula [*Hopkins*, 1963; *Swanson et al.*, 1981; *Wood and Kienle*, 1990; *Moll-Stalcup*, 1994]. However, most of the volcanism in the Bering Sea region is much younger and extends from circa 6 Ma to fairly recent times [*Wood and Kienle*, 1990; *Moll-Stalcup*, 1994, 1996; *Beget et al.*, 2003; *Winer et al.*, 2004]. The province consists of a number of large late Cenozoic volcanic fields composed of broad plains or shield volcanoes of voluminous lava flows overlain by steep cones and/or maars of undersaturated, highly alkaline basaltic magma [*Hoare and Coonrad*, 1980; *Davis et al.*, 1994; *Moll-Stalcup*, 1994]. Most of the basaltic volcanism in the province occurs in close association with east-west normal faulting [*Hoare et al.*, 1968; *Swanson et al.*, 1981].

[4] Several workers [e.g., *Nakamura et al.*, 1977; *von Drach et al.*, 1986; *Swanson et al.*, 1987] describe rocks of the BSVP as "back-arc" basalts because of their location behind the Aleutian arc. On the basis of major and trace element characteristics, however, *Moll-Stalcup* [1994] argued that BSVP basalts originated from a source similar to that of ocean island basalts (OIB). *Swanson et al.* [1981] on the other hand used the diffuse and widespread character of the volcanism in the BSVP to invoke a continental rift environment, particularly for the most closely studied area of Seward Peninsula. *Menzies and Murthy* [1980], *Roden et al.* [1984] and *Moll-Stalcup* [1996] asserted that at least

[1]Department of Geological Sciences, University of Michigan, Ann Arbor, Michigan, USA.

0148-0227/07/2006JB004452$09.00

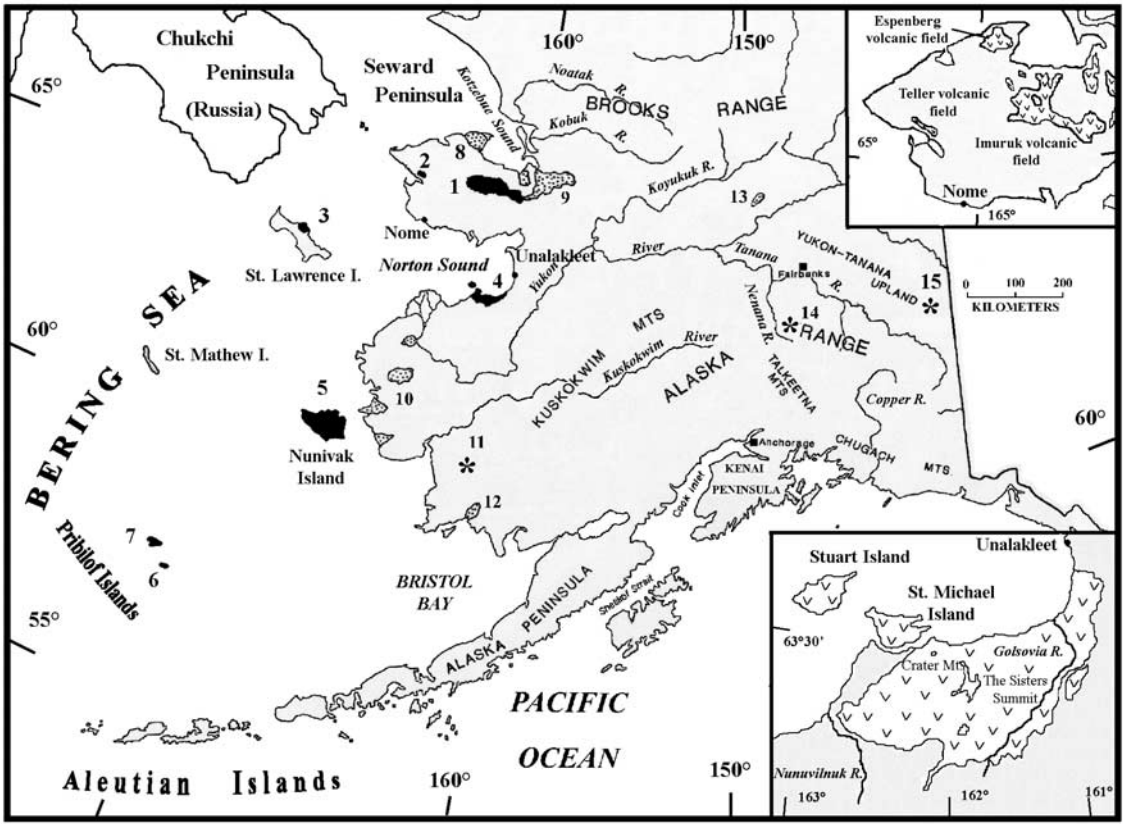

Figure 1. Location map of late Cenozoic volcanic fields and individual volcanoes in Alaska; modified from *Hoare and Coonrad* [1980], and *Moll-Stalcup* [1994]. Legend: 1, Imuruk volcanic field; 2, Teller volcanic field; 3, Kookooligit Mountains of St. Lawrence Island; 4, St. Michael volcanic field; 5, Nunivak Island; 6, St. George Island; 7, St. Paul Island; 8, Espenberg volcanic field; 9, Koyuk-Buckland volcanic field; 10, Yukon Delta volcanic region; 11, Flat Top Mountain volcano; 12, Togiak volcanic field; 13, Fort Hamlin Hills volcanic field; 14, Buzzard Creek maars; 15, Prindle volcano. Black fields indicate location of volcanic rocks dated by $^{40}Ar/^{39}Ar$ chronology in the present study; dotted outlines represent volcanic fields not yet dated by the authors; asterisks represent individual volcanoes. More detailed maps of Seward Peninsula (top) and St. Michael volcanic field (bottom) are given as inserts.

some of the magmatism in the supposed rift was derived from a veined lithospheric mantle.

[5] Each of these models, however, has challenges to overcome. The back-arc model is challenged by the fact that volcanism in the province is not restricted to a well-defined spreading rift axis and indeed covers an area anywhere from 250 to >1200 km inboard from the Aleutian arc (Figure 1). Moreover, it remains to be demonstrated whether typical back-arc rock compositions, generally dominated by a range from normal mid-ocean ridge basalts (NMORB) to arc tholeiites [*Saunders and Tarney*, 1984] are well represented anywhere in the BSVP. As for the hot spot model, no trace with clear age progression from one end of the belt to the other has been conclusively established, and this is indeed part of the justification for the $^{40}Ar/^{39}Ar$ dating study presented here. The weakness of continental rift models is that proponents did not address the possibility of a large plume head even if the surface expression of the tectonic setting is that of a continental rift.

[6] In this study, we have used the laser probe $^{40}Ar/^{39}Ar$ technique to date 35 individual bulk rock samples from 7 different volcanic fields throughout the eastern sector of the BSVP (Figure 1) to refine our understanding of its eruption history. We have also used these results, combined with new volume estimates, to compute eruption rates through time for the largest of the exposures in this volcanic province.

1.2. Volcanic Rock Compositions

[7] Late Cenozoic volcanic fields in the BSVP are dominated by alkali-olivine basalt and tholeiite (95–97%), with basanite, tephrite, hawaiite, and nephelinite adding up to only 3–5% [*Moll-Stalcup*, 1994]. Alkalic and subalkalic basalts (SiO_2 = 38–45 wt %; $Na_2O + K_2O$ = 3.0–7.5 wt %) dominate over tholeiites, broadly with total alkalis decreasing with increasing SiO_2, a characteristic interpreted to represent varying degrees of partial melting of the source at high pressure. Most of volcanic rocks have Mg # [100*Mg/(Mg + Fe)] greater than 65 and many contain ultramafic xenoliths, which together suggest that the magmas are close in composition to the primary melts of mantle peridotite and have experienced little (if any) residence time in shallow magma chambers.

2. The $^{40}Ar/^{39}Ar$ Chronology

2.1. Methods

[8] The samples we have analyzed were crushed with a hardened steel mortal and pestle, and then matrix particles

in the range of 150–250 μm were separated by sieving followed by washing in super de-ionized water. Adopting the approach of *Nicolaysen et al.* [2000], we undertook $^{40}Ar/^{39}Ar$ measurements either on aphyric lavas, or in cases where plagioclase phenocrysts were present, removing them mechanically from the desired basaltic groundmass before further processing of the samples. This was particularly amenable to producing precise ages in the Bering Sea volcanic rocks because of the contrast in K_2O concentrations with the matrix at $\geq$1.5–2.0 wt % and plagioclase at $\leq$0.9 wt %. Approximately 10 mg of material were used per sample. Duplicates of each sample were packaged in pure Al foil before insertion into evacuated quartz tubes for irradiation in the Phoenix Memorial Nuclear Reactor at the University of Michigan. Neutron flux variation (*J*) was measured using the biotite standard from the Fish Canyon Tuff (split 3) and the age used for this standard was calibrated earlier using hornblende standard MMhb-1. The error-weighed mean of five analyses of biotite from the Fish Canyon Tuff, assuming an age of 520.4 Ma for MMhb-1, was 27.99 ± 0.04 Ma (2σ). This value is satisfyingly close to the age of 28.02 Ma found for Fish Canyon Tuff sanidine by *Renne et al.* [1994]. All age estimates include propagated uncertainties in the value of the neutron flux monitor *J*.

[9] Subsequent to irradiation, the sample packets were opened and the whole rock grains were placed into 2 mm diameter wells in a copper disk, and were then individually step heated at increasing levels of laser power, a procedure that mimics temperature-calibrated step heating in the tantalum furnace. The details of the Ar isotope analyses are similar to those reported by *Hall and Farrell* [1995]. All analyses were corrected for fusion system blank levels at the five Ar mass positions. Blanks were run every three to five analyses, and these were approximately 1×10^{-13} mL STP at mass 36 and 3×10^{-11} mL STP at mass 40. The raw analytical data are given in the auxiliary material.[1]

2.2. Elemental Compositions and $^{40}Ar/^{39}Ar$ Ages

[10] We present 35 new $^{40}Ar/^{39}Ar$ age determinations among which, 12 of the samples have good agreement between total gas, plateau, and isochron ages. Four of the 19 samples for which both plateau and isochron ages have been determined, there is good concordance (Table 1). For the remaining 14 samples, plateau and isochron ages are not concordant at the 95% confidence level. The initial $^{40}Ar/^{36}Ar$ ratios derived from the intercepts on the isochron diagrams are very close to the atmospheric value (295.5). This implies a general lack of excess argon, possibly because of the high temperature of eruption and fluidity of the magma, both facilitating degassing of any magmatic Ar and rapid equilibration with the atmosphere. Ages younger than 100 ka have substantially large errors (Table 1), likely reflecting the spread in the $^{40}Ar/^{39}Ar$ values which are too limited to allow precise determination of the initial $^{40}Ar/^{36}Ar$ ratio from the isochron diagrams. Total gas age always has to be used with caution because this approach is at the mercy of the possible presence of xenocrystic material and secondary alteration [*Frey et al.*, 2004]. In cases where there is good agreement between plateau and isochron ages, we have no statistical basis to choose one over the other. The data processing approach yielding the smaller error has been the one adopted in the discussions presented here.

[11] Cited alongside the $^{40}Ar/^{39}Ar$ results as relevant, but the subject of a geochemical paper in preparation, are selected major oxide data for the whole rock samples we have dated. These were obtained by X-ray fluorescence (XRF) spectrometry at Michigan State University using the methods described by *Hannah et al.* [2002].

2.2.1. Imuruk Volcanic Field

[12] *Hopkins* [1963], *Wood and Kienle* [1990], and *Moll-Stalcup* [1994, 1996] were the first to describe the extent and the ages of Cenozoic volcanism of the Imuruk volcanic field (Figure 1), which they divided into the Imuruk Volcanic Series, Gosling Volcanic Series, and the Camille and Lost Jim lava flows. We report here some new $^{40}Ar/^{39}Ar$ ages that improves our understanding of the eruption histories of these eruptives in order to bracket the duration of magmatic activity in the area. The Imuruk Volcanic Series are composed of olivine alkaline basalts with well-crystallized groundmass containing small olivine phenocrysts estimated to be up to 5–7 vol %. The basalts have uniform SiO_2 (43.3–43.6 wt %), high and somewhat variable MgO (8.4–10.4 wt %), but relatively low total alkalis ($Na_2O + K_2O$ = 4.3–6.3 wt %). Sample VB-16 from Virginia Butte within the Imuruk Volcanic Series yields a $^{40}Ar/^{39}Ar$ total gas age of 6.03 ± 0.12 Ma, plateau age 6.07 ± 0.09 Ma and isochron age of 6.10 ± 0.11 Ma (Figure 2a and Table 1). Sample SB-4 from Skeleton Butte also from the Imuruk Volcanic Series, gives ages of 5.54 ± 0.05 Ma (total gas), 5.22 ± 0.05 Ma (plateau), and 5.30 ± 0.09 Ma (isochron; Figure 2d and Table 1). These two eruption events (at circa 6.1 Ma and 5.2 Ma) mark the oldest and youngest eruptions in the Imuruk Volcanic Series, now limited to only about 1 million years, abrogating earlier suggestions of volcanism in the series being as young as 2.2 Ma [*Hopkins*, 1963; *Moll-Stalcup*, 1994].

[13] Our attempts to use the $^{40}Ar/^{39}Ar$ method to date the younger basalts of the Camille and Lost Jim lava flows did not meet with much success, yielding ages close to zero (not reproduced here) for lack of any appreciable radiogenic Ar. We have interpreted these results to mean that the Camille and Lost Jim lava flows are too young to be dated with the $^{40}Ar/^{39}Ar$ method, and have just embarked on the process of dating them using the ^{14}C method.

2.2.2. Teller Volcanic Field

[14] Several basaltic lava flows, three remnant volcanic necks and up to 30 vents [*Wood and Kienle*, 1990] comprise the small Teller volcanic field, estimated to have an area of ~120 km^2 (Figure 1). The rocks have a dark gray, well-crystallized groundmass containing small olivine (7–10 vol %) and augite (up to 5–7 vol %) phenocrysts. These rocks have an alkaline olivine basaltic composition, similar to those from the Imuruk volcanic field (SiO_2 = 43.3–44.6 wt %; MgO = 8.57–10.11 wt %; and total alkalis (Na_2O+K_2O) = 4.92–6.17 wt %). Our new $^{40}Ar/^{39}Ar$ data for three samples from the Teller area (TLR-2, TLR-11 and TLR-12; Figure 3 and Table 1) produce total gas ages of 3.41 ± 0.03 Ma to 3.58 ± 0.05 Ma, but a wider range is isochron ages between 3.29 ± 0.09 Ma and 3.51 ± 0.06 Ma. Only TLR-12 produces a plateau age, with 61% of the gas released, at 3.60 ± 0.07 Ma. These results indicate that

[1]Auxiliary materials are available at ftp://ftp.agu.org/apend/jb/2006jb004452.

Table 1. The ^{40}Ar/^{39}Ar Ages ($\pm 1\sigma$) for Cenozoic Volcanic Rocks of the Eastern Bering Sea Volcanic Province[a]

Sample	Total Gas Age, Ma	Plateau Age, Ma	Plateau MSWD	Plateau Percent ^{39}Ar	Isochron Age, Ma	MSWD	(^{40}Ar/^{36}Ar)$_i$	Points Fitted
Imuruk Lake Area								
VB-16	6.03 ± 0.12	6.07 ± 0.09	0.716	100	6.10 ± 0.11	0.772	293.6 ± 3.3	A
VB-17	5.83 ± 0.06	5.75 ± 0.05	0.888	100	5.79 ± 0.06	0.741	302.0 ± 4.2	A
SB-8	5.33 ± 0.06	5.41 ± 0.05	0.467	80	5.33 ± 0.10	0.938	266.7 ± 9.5	P
SB-4	5.54 ± 0.05	5.22 ± 0.05	1.175	62	5.30 ± 0.09	1.196	282.6 ± 12.4	P
Teller Area								
TLR-12	3.58 ± 0.05	3.60 ± 0.07	0.982	61	3.51 ± 0.06	0.992	294.1 ± 0.9	P
TLR-2	3.48 ± 0.05	n/a	n/a	n/a	3.30 ± 0.04	0.951	297.6 ± 0.5	A
TLR-11	3.41 ± 0.03	n/a	n/a	n/a	3.29 ± 0.09	0.867	323.7 ± 9.3	A
St. Lawrence Island								
KB-11M	1.32 ± 0.02	1.22 ± 0.02	0.989	70	1.22 ± .0.05	0.997	285.1 ± 10.6	P
St. Michael Volcanic Field								
SIS-6	0.80 ± 0.03	0.61 ± 0.03	1.032	85	0.60 ± 0.13	1.171	294.0 ± 6.4	P
SIS-15	0.68 ± 0.04	0.58 ± 0.03	1.124	90	0.54 ± 0.03	1.105	297.2 ± 1.5	P
CRT-2	0.39 ± 0.02	0.41 ± 0.02	0.514	73	0.41 ± 0.04	1.616	289.8 ± 3.7	P
CRT-9	0.37 ± 0.02	0.36 ± 0.01	0.884	78	0.37 ± 0.04	0.964	295.5 ± 4.9	A
STM-7	0.27 ± 0.06	0.25 ± 0.04	0.755	100	0.26 ± 0.07	0.815	294.0 ± 14.3	A
STM-5	0.16 ± 0.05	0.18 ± 0.04	1.551	100	0.20 ± 0.06	0.879	290.6 ± 6.8	A
STM-2	0.15 ± 0.05	0.13 ± 0.04	0.770	86	0.16 ± 0.06	0.791	289.6 ± 8.0	P
STM-3	0.10 ± 0.07	0.12 ± 0.06	1.166	78	0.08 ± 0.06	1.721	298.0 ± 8.2	P
KON-1	0.08 ± 0.05	0.06 ± 0.04	0.749	100	0.04 ± 0.15	1.125	284.4 ± 12.9	A
Nunivak Island								
NVE-6	0.70 ± 0.08	0.71 ± 0.05	1.052	100	0.68 ± 0.10	1.097	310.6 ± 2.1	A
NVA-15-1	0.34 ± 0.07	0.26 ± 0.07	1.351	96	0.30 ± 0.09	0.517	297.6 ± 1.8	P
NVB-4-2	0.20 ± 0.07	n/a	n/a	n/a	n/a	n/a	n/a	n/a
NVF-9	0.19 ± 0.06	0.21 ± 0.04	0.921	95	0.25 ± 0.07	0.592	288.9 ± 3.6	P
NVC-18	0.15 ± .0.06	0.16 ± 0.05	0.768	100	n/a	n/a	n/a	n/a
St. George Island								
SGC-10	2.60 ± 0.02	2.46 ± 0.02	2.980	73	2.42 ± 0.04	0.338	299.7 ± 36.6	P
SGB-2	2.07 ± 0.04	2.05 ± 0.03	0.484	93	2.01 ± 0.05	0.530	296.4 ± 6.4	P
SG-2	1.75 ± 0.07	1.75 ± 0.07	1.079	81	1.75 ± 0.16	1.182	295.6 ± 17.2	P
SG-3	1.68 ± 0.05	1.61 ± 0.05	1.147	62	1.64 ± 0.07	0.759	292.1 ± 9.7	P
SG-5	1.42 ± 0.06	1.64 ± 0.05	1.003	75	1.58 ± 0.06	0.940	307.6 ± 8.9	P
SG-6	1.58 ± 0.06	1.57 ± 0.05	0.654	100	1.60 ± 0.07	0.360	296.1 ± 8.7	A
SG-4	1.52 ± 0.09	1.47 ± 0.05	0.874	100	1.44 ± 0.07	1.500	299.2 ± 2.9	A
SG-1	1.41 ± 0.04	1.44 ± 0.04	1.506	100	1.37 ± 0.07	1.549	302.3 ± 6.9	P
St. Paul Island								
SPC-5	0.41 ± 0.12	0.40 ± 0.09	1.084	79	0.42 ± 0.09	0.965	254.8 ± 36.9	A
SPD-1	0.30 ± 0.15	n/a	n/a	n/a	n/a	n/a	n/a	n/a
SPB-1	0.14 ± 0.10	0.17 ± 0.09	0.402	78	0.18 ± 0.09	0.735	277.8 ± 13.4	A
SPB-5	0.21 ± 0.11	0.15 ± 0.07	0.614	89	0.16 ± 0.09	0.632	283.0 ± 14.6	P
SPE-1	0.14 ± 0.10	n/a	n/a	n/a	0.13 ± 0.13	1.897	281.1 ± 69.9	A

[a]Plateaus are defined using the method of *Fleck et al.* [1977]; that is, they consist of at least three consecutive heating steps, which overlap within 2σ uncertainties and represent at least 50% of the total ^{39}Ar released. Fits denoted P are based on the points defining the plateau, and those marked A are based on all points. The choice of A or P is driven largely by the initial ^{40}Ar/^{36}Ar ratios. Plateau ages are error weighted averages with scatter included in the error estimate. The mean square weighted deviation (MSWD) measures the quality of the line fit, and an MSWD of 1.0 correlates with a line perfectly defined by the data. All correlation diagrams with MSWD >2 are considered error chrons; n/a, not applicable.

volcanic activity in the Teller region was of very short duration, in all likelihood not exceeding 300–350 thousand years. There is no indication of any volcanism in this area that is younger than 3.3 Ma.

2.2.3. St. Lawrence Island

[15] Quaternary basalt cinder cones and lava flows form a large shield volcano, over 500 m high, in the north central part of St. Lawrence Island (Kookooligit Mountains). The overwhelming majority of the volcanic rocks at this locality are alkali-olivine basalt, with only subordinate amounts of olivine tholeiite, basanite and minor nephelinite [*Patton and Csejtey*, 1971; *Moll-Stalcup*, 1994, 1996]. The alkaline basalts are characterized by a high Mg # (61–64), with MgO = 7.9–12.2 wt %, low silica (SiO_2 = 44.8–46.2 wt %), and high total alkalis (Na_2O+K_2O = 3.8–7.7 wt %) [*Moll-Stalcup*, 1996]. Only one sample (KB-11M) of alkaline olivine basalt has been dated in our study using the ^{40}Ar/^{39}Ar method obtaining a total gas age of 1.32 ± 0.02 Ma, plateau age of 1.22 ± 0.02 Ma, and isochron age of 1.22 ± 0.05 Ma (Figure 4 and Table 1). *Moll-Stalcup* [1994, 1996] produced K-Ar data for this shield volcano which suggest that volcanic activity in the Kookooligit Mountains continued

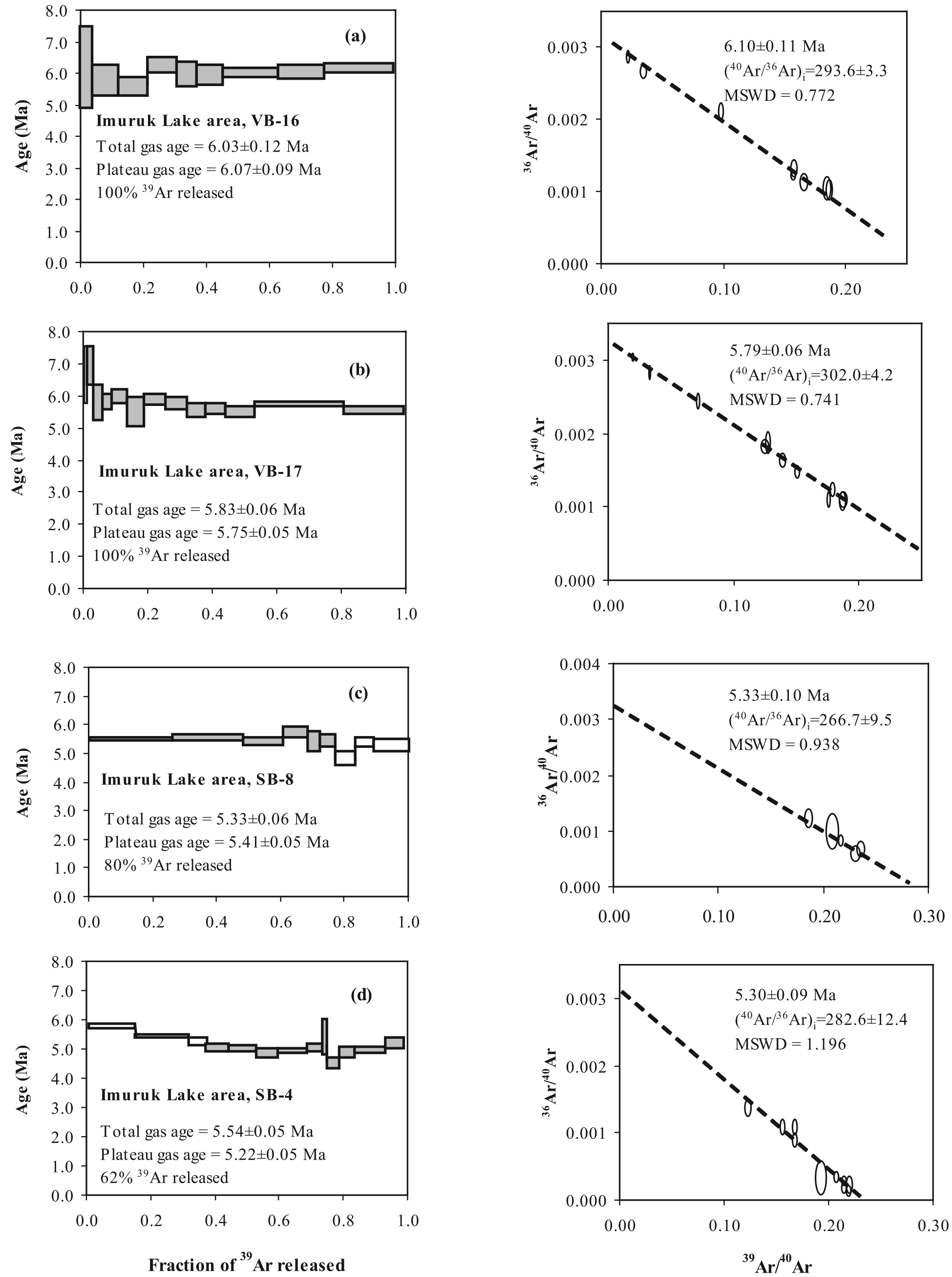

Figure 2. Step-heating spectrum and isochron diagrams for basalt whole rock samples from the Imuruk volcanic field. The age spectra show plateaus defined by at least three consecutive steps with >50% of the total gas released and whose ages agree within 2σ (gray fields). Where plateaus are not available, only total gas ages are taken into consideration (white fields). Inverse isochron diagrams generated by the regression methods of *York* [1969] have been included, whenever possible, to show the integrity of the gas fractions released and the significance of any other gas components besides radiogenic and atmospheric. The $^{36}Ar/^{40}Ar$ intercept reflects the initial $^{36}Ar/^{40}Ar$ of the sample and the age of the sample is calculated from the $^{39}Ar/^{40}Ar$ intercept (the atmospheric $^{36}Ar/^{40}Ar$ = 0.00338, i.e., 1/295.5). The reported age is for the regression line going through the plateau points unless stated otherwise in Table 1.

until 0.24 Ma. Although yet to be verified, combining our $^{40}Ar/^{39}Ar$ data with these published K-Ar ages implies that activity continued in a single shield volcano complex for nearly 1 million years.

2.2.4. St. Michael Volcanic Field

[16] The St. Michael volcanic field completely covers St. Michael and Stuart Islands, and extends inland as far as the Golsovia and Nunuvilnuk rivers (south to southwest from Unalakleet village); a part of the field is submerged beneath Norton Sound (Figure 1). The field consists of more than 50 cones and craters and numerous flat-lying lava flows and tuffaceous layers. We collected samples from the lava flows and volcanic craters on St. Michael Island, and also from several lava and cinder cones on the mainland.

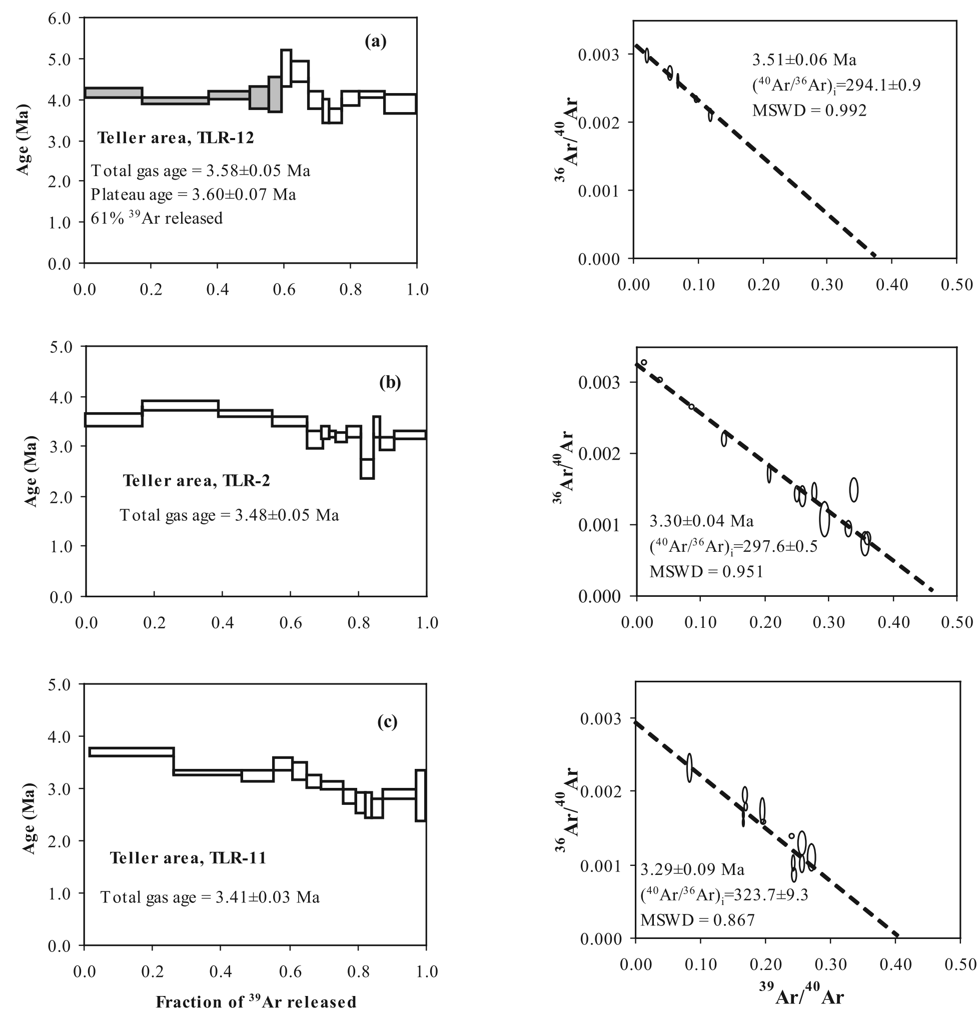

Figure 3. Step-heating spectrum and isochron diagrams for basanite whole rock samples from the Teller volcanic field. For samples TLR-2 and TLR-11, no plateau ages were obtained, making these determinations provisional and subject to verification. The regression lines on the inverse isochron diagrams reflect total gas ages for samples TLR-2 and TLR-11 and the plateau age for sample TLR-12. The area was volcanically active for only a short time (~310 thousand years).

The rocks are rich in aluminum (14.7–15.4% Al_2O_3), but are poor in total alkalis ($Na_2O + K_2O$ = 4.14–4.75%). Silica is moderate (47.9–49.3% SiO_2), and MgO varies from 7.28% to 9.44%. Morphologically in the field, it appears that the mainland sector of the volcanic field has more of the older flows while the nearby offshore islands are composed of the younger rocks.

[17] Dating has identified the oldest rocks in this volcanic field to be in the unnamed small vent located 5 km southwest of The Sisters Summit (0.80 ± 0.03 Ma, total

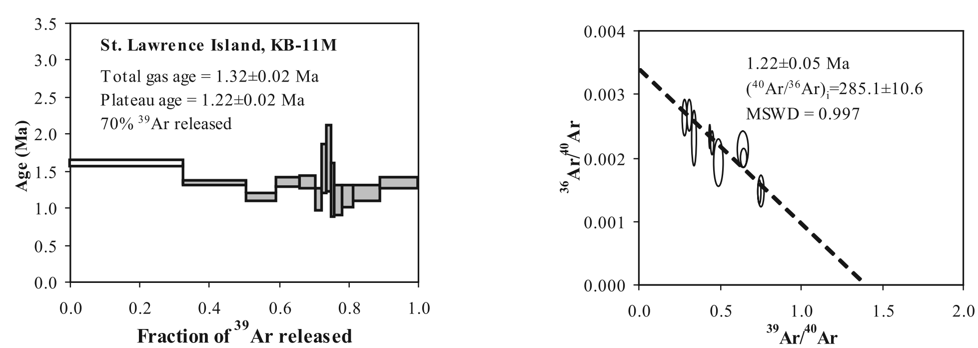

Figure 4. Step-heating spectrum and isochron diagrams for basalt whole rock sample from Kookooligit Mountains of St. Lawrence Island. A very good correlation between the plateau and isochron ages indicates that the eruption of the lava flow dated took place at 1.22 ± 0.05 Ma.

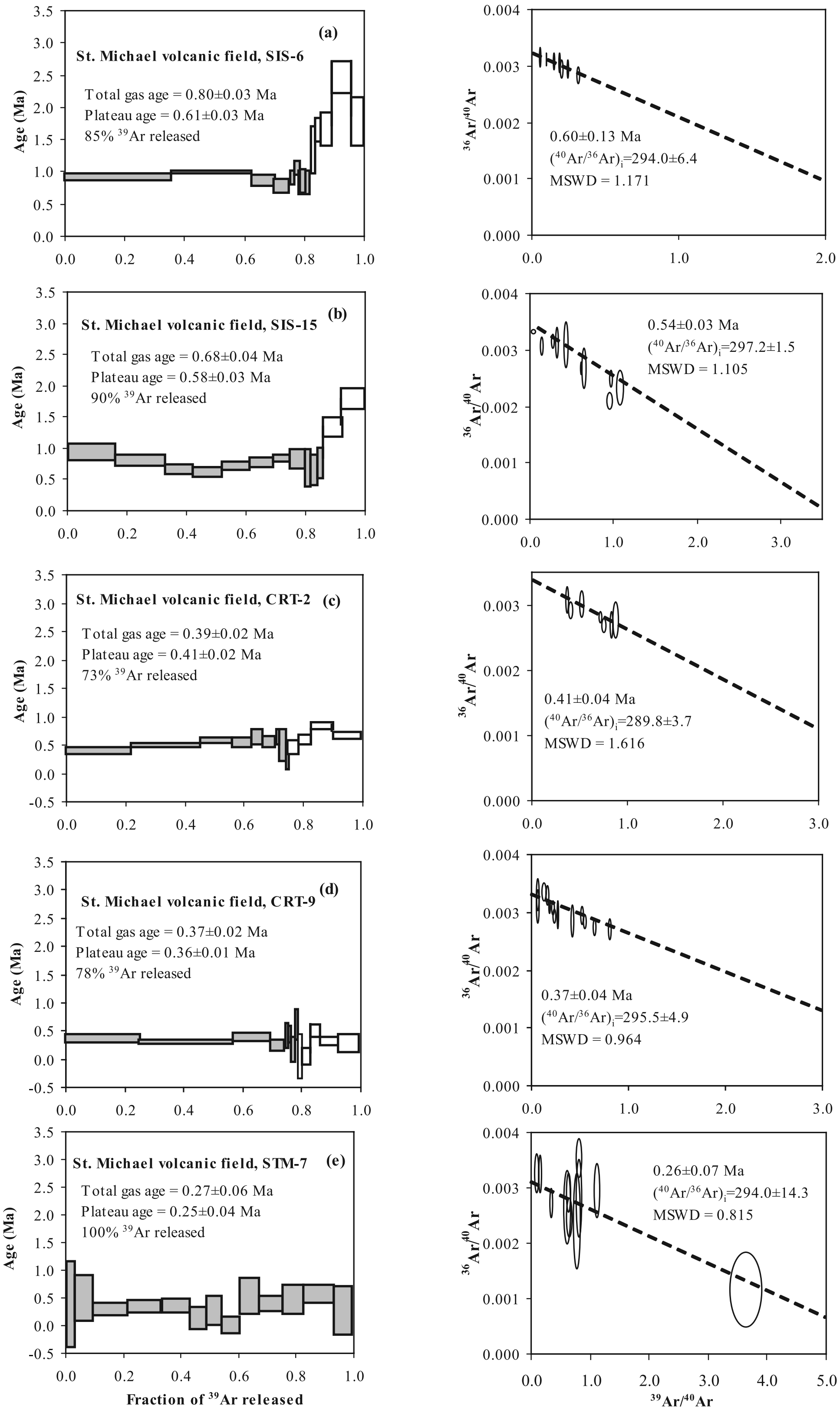
(a)
St. Michael volcanic field, SIS-6
Total gas age = 0.80±0.03 Ma
Plateau age = 0.61±0.03 Ma
85% ^{39}Ar released
0.60±0.13 Ma
(^{40}Ar/^{36}Ar)$_i$=294.0±6.4
MSWD = 1.171
(b)
St. Michael volcanic field, SIS-15
Total gas age = 0.68±0.04 Ma
Plateau age = 0.58±0.03 Ma
90% ^{39}Ar released
0.54±0.03 Ma
(^{40}Ar/^{36}Ar)$_i$=297.2±1.5
MSWD = 1.105
(c)
St. Michael volcanic field, CRT-2
Total gas age = 0.39±0.02 Ma
Plateau age = 0.41±0.02 Ma
73% ^{39}Ar released
0.41±0.04 Ma
(^{40}Ar/^{36}Ar)$_i$=289.8±3.7
MSWD = 1.616
(d)
St. Michael volcanic field, CRT-9
Total gas age = 0.37±0.02 Ma
Plateau age = 0.36±0.01 Ma
78% ^{39}Ar released
0.37±0.04 Ma
(^{40}Ar/^{36}Ar)$_i$=295.5±4.9
MSWD = 0.964
(e)
St. Michael volcanic field, STM-7
Total gas age = 0.27±0.06 Ma
Plateau age = 0.25±0.04 Ma
100% ^{39}Ar released
0.26±0.07 Ma
(^{40}Ar/^{36}Ar)$_i$=294.0±14.3
MSWD = 0.815
Age (Ma)
^{36}Ar/^{40}Ar
Fraction of ^{39}Ar released
^{39}Ar/^{40}Ar

Figure 5

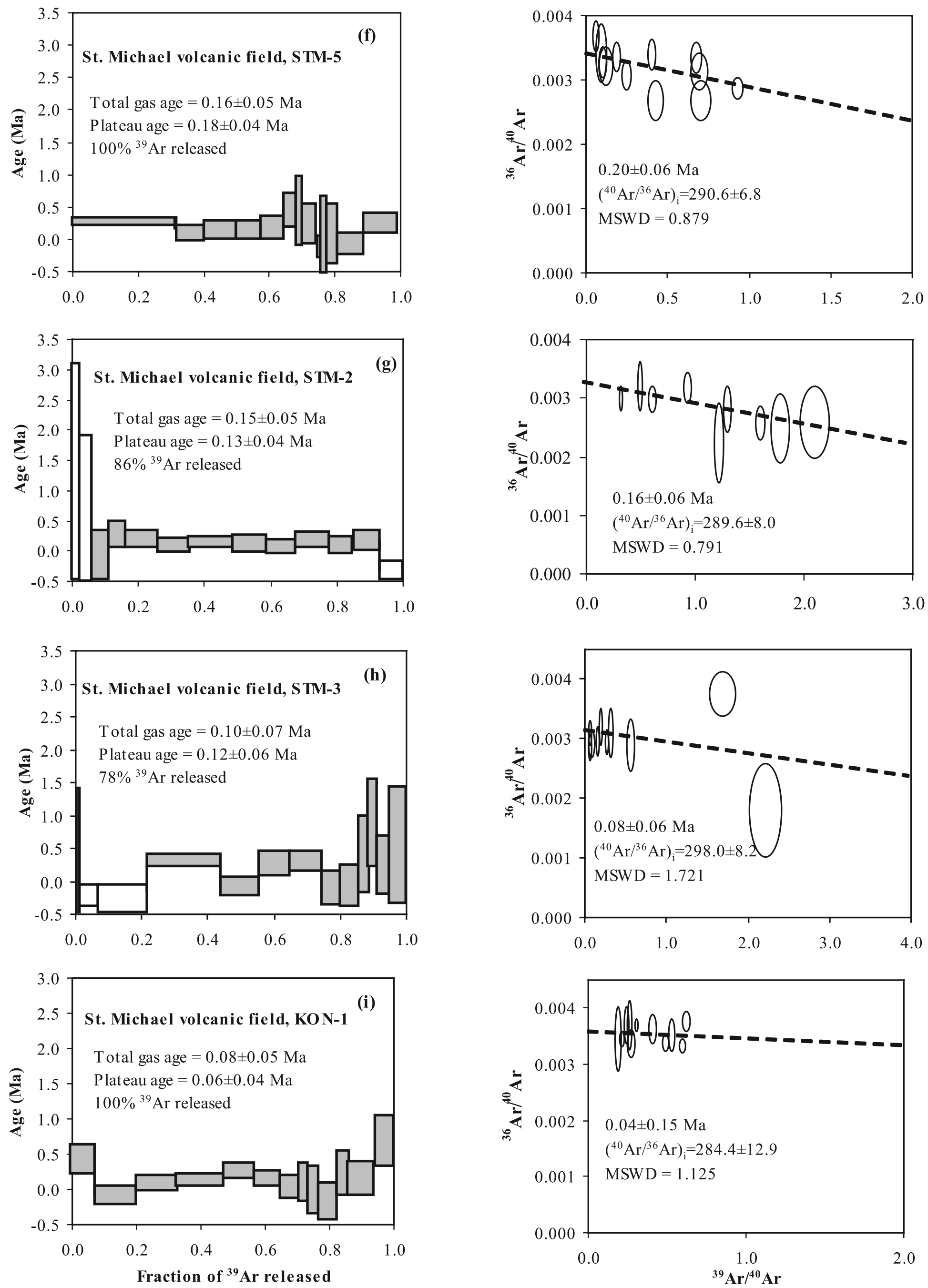

Figure 5. (continued)

gas age; 0.61 ± 0.03 Ma, plateau age; 0.60 ± 0.13 Ma, isochron age; SIS-6; Figure 5a and Table 1). The youngest lavas in this field on the mainland are found at Crater Mountain (0.37 ± 0.02 Ma, total gas age; 0.36 ± 0.01 Ma, plateau age; 0.37 ± 0.04 Ma, isochron age; sample CRT-9; Figure 5d and Table 1). Offshore, the oldest lavas on St. Michael Island (0.28 ± 0.06 Ma, total gas age; 0.25 ± 0.04 Ma, plateau age; 0.26 ± 0.07 Ma, isochron age; sample

Figure 5. Step-heating spectrum and isochron diagrams for basalt whole rock samples from St. Michael volcanic field. Samples SIS-6, SIS-15, CRT-2, and CRT-9 are from the continental part of the volcanic field, and samples STM-7, STM-5, STM-2, and STM-3 are from St. Michael Island. Sample KON-1 is from the southern part of the mainland sector of the volcanic field. Sections of the St. Michael Island volcanic rocks are quite young (<0.25 Ma), whereas volcanic rocks from the mainland sector of the volcanic field erupted between circa 0.61 Ma and circa 0.31 Ma. The youngest rocks (KON-1, circa 0.06 Ma) might belong with the separate volcanic episode. Spectra for samples SIS-6 and SIS-15 exhibit evidence for the presence of a second, Ar-releasing phase, possibly clinopyroxene, or postirradiation ^{39}Ar release.

STM-7; Figure 5e and Table 1) are found in the bluffs on the north shore of the island, near the Stephen Hills volcanic cone from which they originated.

[18] Peak activity on St. Michael Island took place at circa 0.18–0.12 Ma when lavas erupted from several volcanic cones and maars became widely distributed on the island. We dated rocks from one of the volcanic cones (0.16 ± 0.05 Ma total gas age, 0.18 ± 0.03 Ma plateau age, 0.20 ± 0.06 Ma isochron age; sample STM-5; Figure 5f and Table 1); from the main vent of St. Michael Mountain (0.15 ± 0.05 Ma, total gas age; 0.13 ± 0.04 Ma, plateau age; 0.16 ± 0.06 Ma, isochron age; sample STM-2; Figure 5g and Table 1); and from one of the maars (0.10 ± 0.07 Ma, total gas age; 0.12 ± 0.06 Ma, plateau age; 0.08 ± 0.06 Ma, isochron age; sample STM-3; Figure 5h and Table 1).

[19] It appears that an extended period of dormancy followed, only to be succeeded by renewed activity in more recent times, forming several unnamed cinder cones in the central and southern parts of the mainland segment of the volcanic field. One sample from this renewed activity taken from a cinder cone at the southern edge of the field is the youngest rock we have dated so far, challenging the limits of the Ar-Ar dating method due to the low concentrations of radiogenic ^{40}Ar resulting in poor precision and probably accuracy (0.08 ± 0.05 Ma, total gas age; 0.06 ± 0.04 Ma, plateau age; 0.04 ± 0.15 Ma, isochron age; Figure 5i and Table 1). While these data indicate active eruption in the St. Michael volcanic field from circa 0.61 Ma to circa 0.06 Ma, the legends of the aboriginal people include accounts that suggest continued activity into more recent times, when humans had already migrated to North America (i.e., within the past ~10,000 years; presently, the earliest identifiable artifacts are found on Seward Peninsula and have a radiocarbon age of 9070 ± 150 years: 7120 B.C. [*West*, 1981]). We also reported an ethnological account from Eskimo elders: "It was a time when all the mountains were smoking," which suggests that some of the eruptions in the area may have taken place after Eskimo settlements had been established. Inasmuch as the oldest, known Eskimo settlements in western Alaska date back to 200–500 B.C. [*Dumon*, 1987; *Burch and Forman*, 1988], the latest eruptions in the region may be as young as 2000–3000 years old.

2.2.5. Nunivak Island

[20] Nunivak Island, some 50 km off the cost of western Alaska in the Bering Sea, is composed largely of Cretaceous sedimentary rocks upon which Cenozoic volcanic activity has constructed a landscape dominated by broad thin pahoehoe lava flows, cinder cones and maars [*Roden et al.*, 1984; *Wood and Kienle*, 1990]. Exposures are best along sea cliffs and among the very young flows of the eastern part of the island, which is otherwise covered with tundra and shallow lakes. The samples were collected only from volcanic cones and maars in the southeastern corner of the island where massive, dense olivine hyalobasalt and vesicular alkaline olivine basalt are dominant. Overall, the rocks have relatively high Al_2O_3 (14.1–14.3 wt %) and total alkalis ($Na_2O + K_2O$ = 6.9–7.5 wt %), moderate SiO_2 (43.1–44.4 wt %), and low MgO (7.4–8.5 wt %), all rather different compared to the other volcanic rocks we have studied in the BSVP. Sample NVE-6 (Figure 6a and Table 1) represents the oldest flow we have dated on the island, obtaining a total gas age of 0.70 ± 0.08 Ma, a plateau age of 0.71 ± 0.05 Ma and an isochron age of 0.68 ± 0.10 Ma. The youngest lava we have dated on the island (sample NVC-18; Figure 6e and Table 1) yields a total gas age of 0.15 ± 0.06 Ma and a plateau age of 0.16 ± 0.05 Ma; it did not yield an isochron. Collectively, these data show that basaltic volcanism was active in the eastern part of Nunivak Island between circa 0.70 Ma and circa 0.15 Ma.

2.2.6. Pribilof Islands

2.2.6.1. St. George Island

[21] The sea cliffs ringing St. George Island (Figure 1) provide the best exposures of lavas produced during several repeated eruptions, not fewer than seven according to *Wood and Kienle* [1990]. The rocks are olivine-phiric dark gray basanite with finely crystalline groundmass. They have the lowest SiO_2 (38.0–40.2 wt %) and Al_2O_3 (12.4–12.8 wt %) and the highest MgO (10.5–11.0 wt %) concentrations of all the lava samples we have studied. High total alkalis ($Na_2O + K_2O$ = 6.0–6.6 wt %) are also typical for the lavas on St. George Island, qualifying them as alkaline ultramafic rocks. Along the southeastern coast of the island, the basanitic rocks sit directly on peridotite basement exposed in a series of outcrops, providing the opportunity to determine the exact time of the onset of the volcanic activity on the edge of the Bering Sea continental shelf. Our $^{40}Ar/^{39}Ar$ age determinations on the lowermost volcanic layer (Figure 7a and Table 1) give a total gas age of 2.60 ± 0.02 Ma, plateau age of 2.46 ± 0.03 Ma, and an isochron age of 2.42 ± 0.04 Ma, constraining the approximate time that volcanic activity began on the island. We also took samples from the youngest lavas on the island, which crop out near the northern coast. Sample SG-1 (Figure 7h and Table 1) yields a plateau age of 1.44 ± 0.04 Ma and an isochron age of 1.37 ± 0.07 Ma, which are in good agreement with the total gas age of 1.41 ± 0.05 Ma. These data indicate that St. George Island was an active volcano for approximately 1 million years between circa 2.5 Ma and circa 1.4 Ma. Overall, the volcanism appears to have been episodic producing three main eruptions at circa 2.5 Ma, circa 2.0–1.4 Ma, and circa 1.5–1.4 Ma (Table 1).

2.2.6.2. St. Paul Island

[22] Most of St. Paul Island (Figure 1) consists of coalescing small volcanoes, each comprising a central cinder cone built on subdued shield-like sequences of lava flows. Most flows are of the pahoehoe type, but at least three are aa, and alkali olivine basalts dominate [*Barth*, 1956; *Wood and Kienle*, 1990; *Feeley and Winer*, 1999]. Basalts display elevated SiO_2 (44.0–46.2 wt %) and Al_2O_3 (11.7–15.5 wt %), and low MgO (6.3–7.2 wt %) and total alkali ($Na_2O + K_2O$ = 3.6–5.1 wt %) concentrations compared to the other lavas in the BSVP. Unlike St. George Island, there is no basement exposed on St. Paul, making it difficult to determine the exact onset of volcanic activity at this locality. The stratigraphically oldest basalt layer exposed has yielded a total gas age of 0.40 ± 0.12 Ma, plateau age of 0.40 ± 0.09 Ma and an isochron age of 0.42 ± 0.09 Ma (Figure 8a and Table 1). These ages are somewhat younger than the age of 0.54 Ma reported by *Winer et al.* [2004] as marking the onset of volcanic activity on the island. Although our $^{40}Ar/^{39}Ar$ age determinations suggest that the youngest volcanic rocks erupted on the island at circa 0.13 Ma (sample SPE-1, Table 1), *Winer et al.* [2004] showed on the basis of radiocarbon dating of paleosoils that the youngest basalt

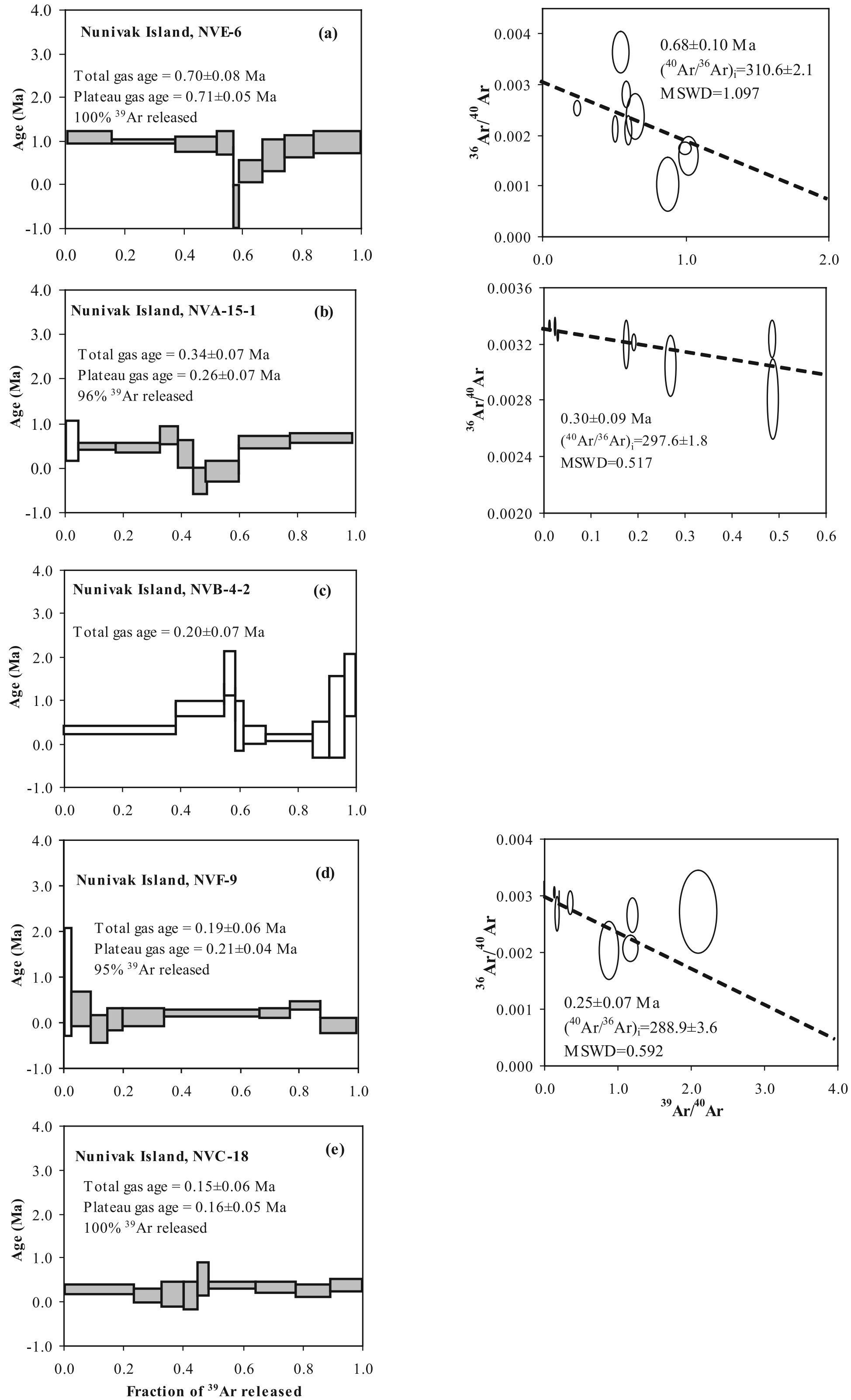

Figure 6. Step-heating spectrum and isochron diagrams for basalt whole rock samples from Nunivak Island. There was long-lived volcanic activity on Nunivak, lasting >550 thousand years (from circa 0.71 Ma for NVE-6 to circa 0.16 Ma for NVC-18). No plateau age was obtained for sample NVB-4-2, and no isochrons were generated for this sample or NVC-18 with which it is spatially associated.

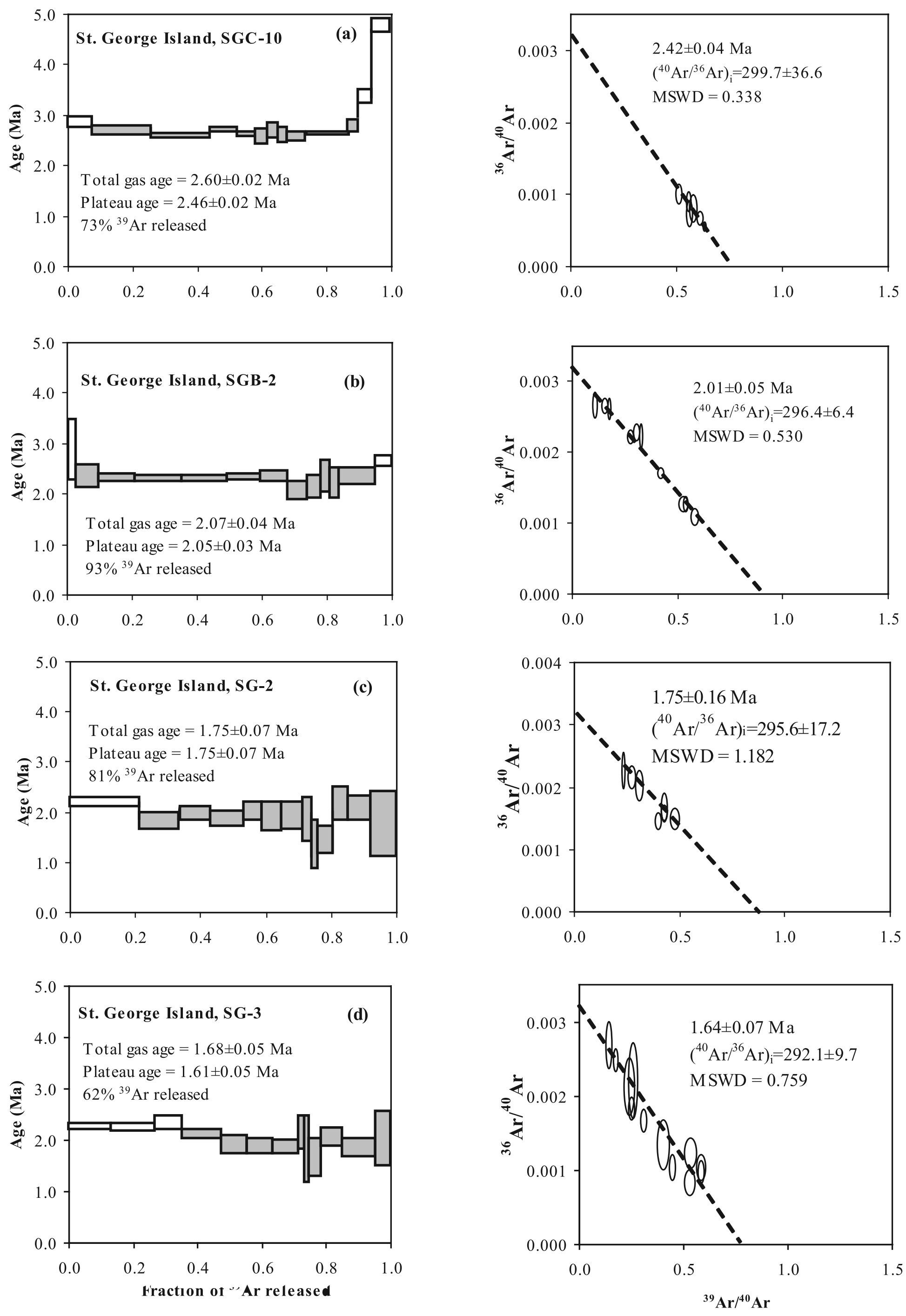

Figure 7. Step-heating spectrum and isochron diagrams for basalt whole rock samples from St. George Island. A very good agreement between plateau gas ages and isochron ages suggests that the volcanic activity on the island took place between 2.46 Ma and 1.44 Ma with probable peaks of activity at circa 2.5 Ma, 2.0–1.7 Ma, and 1.5–1.4 Ma.

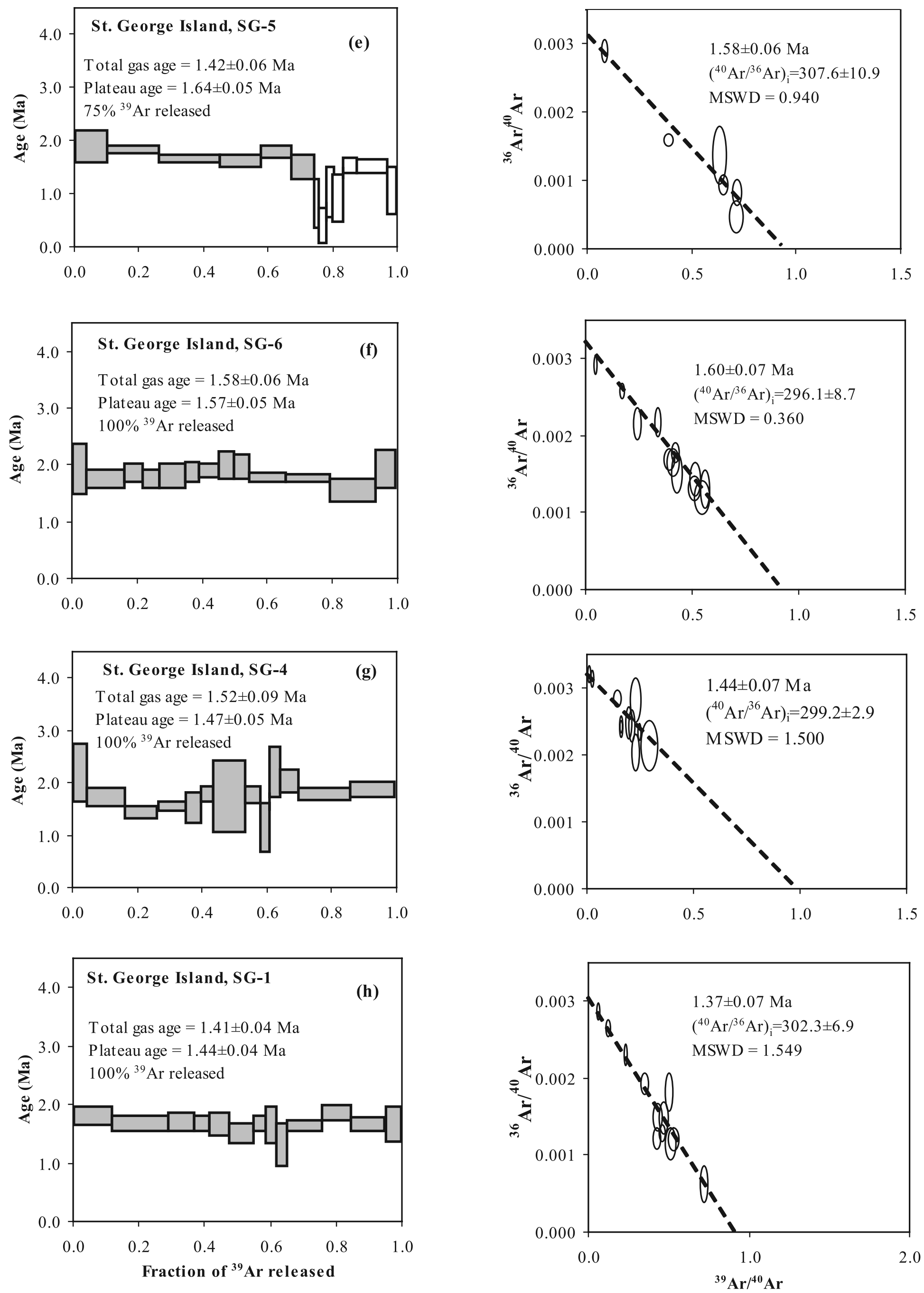

Figure 7. (continued)

flows on St. Paul Island might have erupted as recently as 3230 ± 40 years ago. Therefore, combining their data with ours shows that volcanic activity on the island lasted from circa 400 ka to circa 3 ka. The young age limit to the volcanism on St. Paul suggests that the island may still be active, with potential for future eruptions.

3. Discussion

3.1. Comparison With Previous Results

[23] Previously published eruption ages for the BSVP lavas are mainly restricted to K-Ar determinations, which as ^{40}Ar/^{39}Ar spectrum and isochron ages often indicate, should not in all cases have chronological significance. Nevertheless, the ^{40}Ar/^{39}Ar ages we have reported here (Table 1) are in reasonably good agreement with many of the published K-Ar ages by *Wood and Kienle* [1990], *Davis et al.* [1994] and *Moll-Stalcup* [1994]. Notable differences are largely in the durations of magmatic activity for individual volcanic fields. For example, published eruption ages for the Imuruk volcanic field using the K-Ar method range from 5.8 Ma to 2.2 [*Moll-Stalcup*, 1994], while our new ^{40}Ar/^{39}Ar age determinations give a much narrower range of 6.07–5.22 Ma, with the Camille and Lost Jim lava flows in the same general vicinity being too young to date by the ^{40}Ar/^{39}Ar method.

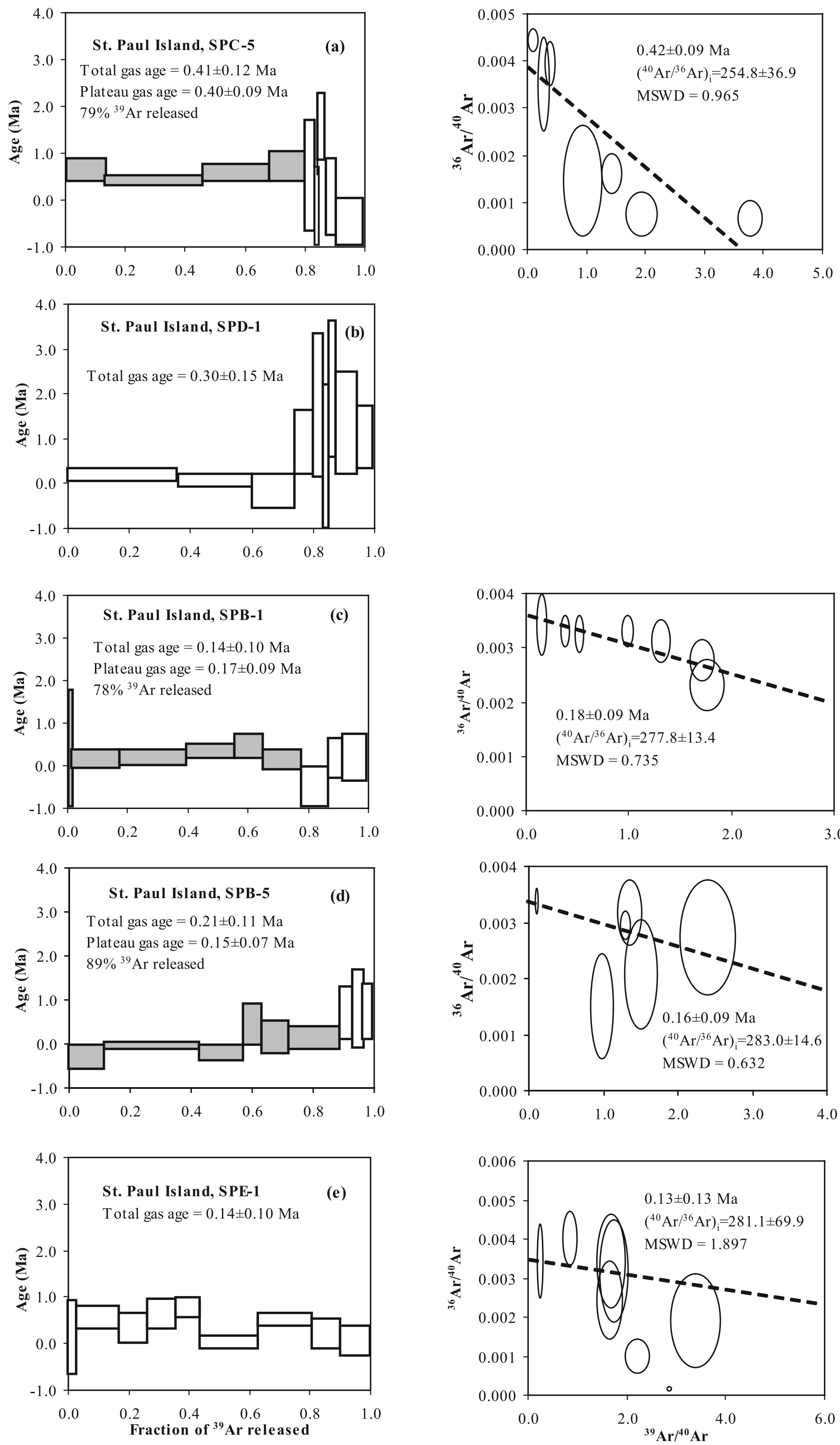

Figure 8. Step-heating spectrum and isochron diagrams for basalt whole rock samples from St. Paul Island. According to data presented here, the island was volcanically active from circa 0.40 Ma to circa 0.13 Ma. Data from *Winer et al.* [2004] suggests that eruptions may have extended into more recent times. Sample SPE-1 did not generate a plateau and sample SPD-1 yielded no isochron or plateau.

Table 2. Calculated Volume of Lava Erupted in the Studied Part of the Bering Sea Volcanic Province

Volcanic Center	Area, km^2	Average Thickness, km	Volume of Exposed Lava, km^3	Sediments in the Sequence, %	Vesicularity, %	Volume of Lava Flows, km^3	Volume of Cones, km^3	Erosion, [a] %	Total Volume of Erupted Magma, km^3
Imuruk volcanic field	1920	0.045	86.4	-	7	80.4	0.001	27	110.1
Teller volcanic field	117	0.020	2.3	-	10	2.1	0.01	22	2.7
St. Paul Island	115	0.065	7.5	10	15	5.7	0.10	15	6.8
St. Paul volcanic field (including the island)	775	0.065	50.4	10	15	38.6	n/a	15	45.3
St. George Island	95	0.100	9.5	3	5	8.8	0.01	20	11.0
St. George volcanic field (including the island)	1165	0.100	116.5	3	5	107.4	n/a	20	134.3
Pribilof Ridge (including St. George Plateau)	2710	0.100	271	3	5	249.7	n/a	20	312.2
Total Pribilof volcanic field[b]	~3485	~0.090	>310	~5	~7	<300. 0	n/a	~15	~360.0
Kookooligit Mountains[c]	830	0.15	96.6	-	10	86.9	0.10	13	99.9
SE Nunivak Island[d]	~650	0.090	58.5	-	10	52.7	0.10	10	58.7
Western St. Michael volcanic field[e]	~1300	0.100	130.0	3	15	107.2	0.05	10	119.2
Total	~8300								~750

[a]Extent of erosion is given in the text and in Figure 9.

[b]Volume calculations for the Pribilof volcanic field (both subaerial and submarine parts) are made on the basis of published data on dredged basalt occurrences (see references) and can be considered as only approximate.

[c]Lava volume calculations for the Kookooligit Mountains have been made assuming a symmetrical truncated cone shape of the mountains.

[d]The authors collected and dated samples only from the southeastern part of Nunivak Island, and are therefore considering only this part in the calculations.

[e]The authors studied only the western part of the field. According to *Wood and Kienle* [1990], the whole field occupies an area of about 3200 km^2.

[24] Moreover, the St. Michael volcanic field thought to have been active between 3.25 and 0.19 Ma based on K-Ar age determinations [*Wood and Kienle*, 1990], is now shown to have been active only between 0.61 Ma and 0.06 Ma according to our ^{40}Ar/^{39}Ar age data (Table 1). It is possible that some of these differences may reflect sampling biases as our work in the St. Michael area was limited by helicopter range to only the central and island sections of the volcanic field. However, for the Teller region where fresh exposures that can be sampled easily are limited to a few remnant volcanic necks, our ^{40}Ar/^{39}Ar age determinations are older (3.60–3.30 Ma, Table 1) than those obtained by the K-Ar method (2.9–2.5 Ma [*Moll-Stalcup*, 1994]).

[25] On Nunivak Island, the range of the eruption ages obtained by the ^{40}Ar/^{39}Ar method is much narrower (0.71–0.16 Ma, Table 1) compared to the ages obtained by K-Ar method (from 6.1 Ma to 0.0 Ma [*Wood and Kienle*, 1990; *Moll-Stalcup*, 1994]). It is possible that some of these differences are also due to sampling biases, but as *Moll-Stalcup* [1994] did not provide any key details about the K-Ar age analyses, more direct comparisons with our data are not possible. What is clear from all the data available now is that the Being Sea Volcanic Province has been intermittently active since circa 6 Ma, and may essentially still be active today.

3.2. Volume of Erupted Magma

[26] Modern estimates of eruption volumes are calculated using digital elevation models (DEMs) [e.g., *Rowland et al.*, 1999; *Stevens et al.*, 1999; *Lu et al.*, 2004], with supporting detailed lava flow mapping and age control far more complete than currently available in the BSVP. Because a large number of lava flows in the BSVP remain undated and unmapped in detail, our attempts to estimate eruption volumes at this stage do not require the state-of-the-art approach but do indeed yield reasonable estimates for selected areas simply from straightforward modeling based on topographic maps and geometric simplification of features we have dated well. In the absence of high-precision DEMs, the eruptive volumes might be calculated by multiplying the areal extent of each lava field by the average thickness, estimated at several points along the edges where cross sectional views are accessible. Because the BSVP is composed of lava fields that are hundreds of square kilometers in an area of poor accessibility, it is impossible to calculate lava areas and volumes without some error. We have based our lava volume estimates on tracing flow margins onto U.S. Geological Survey (USGS) topographic maps (scale 1:63,360 and 1:250,000) with the use of Google Earth images and then calculating the flow thickness from the contour intervals (either 100 feet or 50 feet, 30 m or 15 m). The thickness estimates were made at equal intervals along the margins of flows, and then averaged. The volume of each flow was then calculated from its average thickness and area. Note that the thickness of the flow along the edges is generally smaller than in the center, which means that our calculations may be underestimates, and therefore suggested volumes only minimum values. Because most lava flows were erupted on relatively flat and smooth topography, our volume estimations should not be wildly off the mark, and instead have reasonable errors. Following the approach by *Hasenaka and Carmichael* [1985], we are estimating our volume calculation errors to be within ± 20%.

3.2.1. Exposed Lava

[27] Volcanoes in the Pribilof Islands provide the best erupted lava volume estimates because of the superb exposures and easy access for sampling to determine ages. St. George Island has an area of 95 km^2 and neighboring St. Paul Island one of 115 km^2. Average total thicknesses for the basaltic flows on St. George Island and St. Paul Island are 100 m and 65 m, respectively [*Barth*, 1956; *Feeley and Winer*, 1999; *Winer et al.*, 2004; authors' observations]. The total volume of the basaltic flows exposed on these two islands is therefore estimated to be about 17 km^3 (Table 2). However, the total volume of lava in the entire Pribilof volcanic region must be much larger, inasmuch as Cenozoic basalts similar to those from the islands have been documented to exist around the islands themselves, and along the Pribilof Ridge stretching northwestward from St. George Island [*Comer et al.*, 1987;

Davis et al., 1994; *Winer et al.*, 2004]. The St. Paul and St. George volcanic fields are separated from each other by the deep St. George graben, a northwest-southeast trending structure filled with sediments [*Comer et al.*, 1987], suggesting that treating these as two separate volcanic fields is not outlandish. We estimate the combined exposed and submarine sections of the St. Paul volcanic field to be $\sim$775 km^2, using topographic and bathymetric maps, and magnetic anomaly data [*Comer et al.*, 1987; *Godson*, 1994; *Marlow et al.*, 1994]. Using similar approach, we estimated that a total area of the exposed and submerged sections of St. George volcanic field is $\sim$1165 km^2. Similarly, the whole area occupied by the Pribilof Ridge (including St. George volcanic field) might reach $\sim$2700 km^2. Combining the exposed and submarine sections of the entire Pribilof volcanic region yields an area of $\sim$3500 km^2. If the average thickness of the basalt flows throughout this entire region is similar to that on St. George and St. Paul Islands (assuming that the lavas erupted onto paleotopographic surfaces), then the total volume of lava in the area might be slightly more than 310 km^3 (Table 2).

[28] The late Cenozoic shield volcano that makes up the Kookooligit Mountains on St. Lawrence Island, constructed on a Paleozoic to Tertiary complex of undifferentiated volcanic, plutonic, and sedimentary rocks, covers an area of about 830 km^2 and is at least 150 m thick, all of it exposed [*Patton and Csejtey*, 1971, 1980; *Moll-Stalcup*, 1994]. Numerous volcanic cones ($\sim$70 [*Moll-Stalcup*, 1994]) might have comprised up to 0.1–0.2 km^3 of the erupted rocks. Because the Kookooligit volcanic complex has an edifice that is roughly conical in shape, we used an equation for the volume of a symmetrical, truncated cone (see below) to estimate the lava volume, which is a little less than 100 km^3.

[29] The exposed part of the Imuruk volcanic field covers an area of about 1920 km^2 with an average combined thickness for multiple lava flows of about 45 m [*Hopkins*, 1963; this work]. Therefore the total exposed volume of this volcanic field is $\sim$85 km^3. Covering an area of 117 km^2, the nearby Teller volcanic field is the smallest of the ones we have studied. With an average thickness of $\sim$20 m, its estimated exposed lava flow volume is only $\sim$2.3 km^3. Both Imuruk and Teller volcanic fields have small volcanic necks and several vents that protrude above the lava flows, but these add only minimally to the total volume of the rocks.

[30] Volume estimations for the rest of the volcanic fields we have studied in the BSVP are more challenging, and are therefore presented only as provisional values. For example, the sampled southeastern corner of Nunivak Island consists of several lava flows and about 30 volcanic cones, necks and maars covering an area of $\sim$650 km^2 and averaging a thickness of $\sim$90 m [*Wood and Kienle*, 1990; *Moll-Stalcup*, 1994], which computes to a volume of $\sim$60 km^3 (Table 2). Large sections of the island, however, remain unstudied in detail because of either vegetation cover or difficulty in gaining access from settlements.

[31] In another setting, the St. Michael volcanic field (Figure 1) consists of numerous lava flows and about 30 cinder cones, and vents. The subaerial sections of the volcanic field occupies >3200 km^2 [*Wood and Kienle*, 1990], but our helicopter range limited us to the $\sim$1300 km^2 of exposures closest to the coast. We estimate the average thickness of the lavas in the area we visited to be up to 100 m, and therefore the total volume of just the visited area to be up to 130 km^3. The volcanic cones making up the relief that stands out over the flat lava flow plains may add about 0.05–0.1 km^3 to the total volume, which is just a small contribution.

3.2.2. Vesicularity and Erosion Considerations

[32] In order to derive the volume of erupted magma (or dense rock equivalent), a correction is required for the vesicularity of lavas and the extent of their erosion. While lava vesicularity can be computed from field and petrographic observations (i.e., 5–15% for the rocks we have studied), the extent of erosion remains poorly known as there have not been any quantitative assessments in the area utilizing cosmogenic nuclides. Erosion therefore can be estimated only either through comparison with other volcanic provinces or using geomorphologic observations. Importantly, glaciation in the BSVP, at least during the Tertiary and Quaternary, was only sporadic and was restricted to areas of high elevation [cf. *Hamilton*, 1994]. The volcanic fields in the study area are all at low elevation, and therefore glacial erosion was not a factor in this volcanic province. Because of the young age (<1 Ma) of most of the lava flows we have studied, several still retain a youthful morphology, including the ropy structures associated with the surfaces of pahoehoe, while others appear to have lost some material to erosion, particularly around vents, some now exposed as volcanic necks. Fortunately, there are geomorphologic features which can be used to estimate erosional rates in the region. Numerous volcanic cones of different ages are widely scattered throughout the BSVP, and using such parameters as their diameter (D) to height (H) ratios, and slope angles, it is possible to trace the progression of erosion through time. Our observations show that very young (modern) volcanic cones possess a very consistent D/H ratio of 0.25 ± 0.05%. Slope angles are also very stable and steep at about 40°. With time, the D/H ratio and slope angles change toward lower values (Table 3). Provided that the shapes of volcanic edifices can be modeled as symmetrical, truncated cones, we have calculated their volumes using

$$V = (\pi H/12)\left(D_{top}^2 + D_{top}D_{base} + D_{base}^2\right)$$

where V is volume of the truncated cone, π is 22/7 or $\sim$3.14, H is height of the cone, D_{top} is diameter of the upper surface of the cone, and D_{base} is diameter of the cone's base. Using our field observations, data from USGS topographic maps (scale 1:63,360 or larger where applicable), and of the new volcanic eruption ages (Table 1), we have calculated the change in erosion rates with time as illustrated in Figure 9. Because volcanic cones protrude above the more subdued and flat topography of the lava flows, they are more vulnerable to erosion early in the process until they have been smoothed out. Figure 9 shows that up to 50% of the volume of a typical volcanic cone will be destroyed within the first million years, whereas only $\sim$20% of the volume will be eroded away during the 4.5 Ma that follow. It is worth noting, however, that these high erosion rates apply only to youthful volcanic cones. Thereafter, the erosion rates for subdued, partially eroded cones and lava flows are slow,

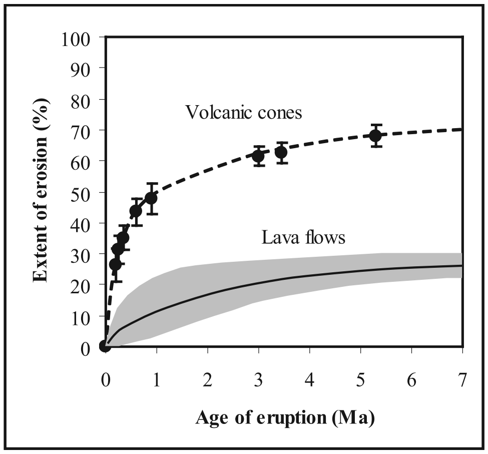

Figure 9. Estimated erosion extents for BSVP volcanic rocks as a function of their eruption ages. The dashed line traces the average extent of erosion for volcanic cones, and the dark solid line traces the average extent of erosion for lava flows; gray field indicates estimated errors for the erosion rates for lava flows. Eruption ages are from data reported here, nearly acquired and yet to be published data by our group, and from *Moll-Stalcup* [1994]. Errors in erosion extent are from Table 4.

essentially invariant, and indistinguishable in the period from 1 Ma to 5.5 Ma (Figure 9). Erosion at this stage can be described by the simple equation of a parabola:

$$y^2 = 2p * x$$

where y is extent of erosion in percent, p is a constant (67 is the best fit for the proposed shape of the curve), and x is the age in Ma. Our calculations are summarized in Table 2. The total volume of Cenozoic lavas erupted throughout the eastern sector of the BSVP is therefore estimated to be about 750 km^3.

3.3. Eruption Rates

[33] Information about the calculated eruption rates is summarized in Table 4 and Figure 10. It is worth reiterating that lavas in the BSVP were erupted during the interval between 6.10 Ma and 0.06 Ma (based on the present ^{40}Ar/^{39}Ar age determinations (Table 1), though a few flows are too young to be dated by the ^{40}Ar/^{39}Ar method). During this interval, about 750 km^3 of magma were erupted across an area estimated to be about 8300 km^2 (Table 2). These values yield an average eruptive flux of ~15 m^3 km^{-2} yr^{-1}, a rate within the range for continental arcs [*Hildreth and Lanphere*, 1994], but much lower (up to 3 orders of magnitude) than the estimated rates for hot spot volcanism [e.g., *Lipman*, 1995; *Nicolaysen et al.*, 2000]. Furthermore, because there is ample evidence for eruptive periods being separated by spells of quiescence, much higher eruption rates can be inferred for individual eruption episodes.

[34] Late Miocene basalts of the Imuruk volcanic field, where about 110 km^3 of lava erupted during a ~850 thousand years period over an area of ~1920 km^2 (Table 2), have yielded the lowest eruption rate, estimated to be ~70 m^3 km^{-2} yr^{-1}. A slightly higher eruption rate of ~75 m^3 km^{-2} yr^{-1} has been calculated for the younger (circa 3.5 Ma) lavas of the Teller volcanic field. The eruption rates increase sharply for Pliocene lavas on St. George Island (~110 m^3 km^{-2} yr^{-1}) and early Pleistocene basalts of Kookooligit Mountains on St. Lawrence Island (~125 m^3 km^{-2} yr^{-1}). The youngest volcanic centers (<0.7 Ma) display even higher rates of eruption (up to ~165 m^3 km^{-2} yr^{-1} for Nunivak Island and St. Michael volcanic fields). However, lava flows on St. Paul Island show a contrary trend. Although young (<500 ka, with some lava flows thought to be even historic [e.g., *Winer et al.*, 2004]), their estimated eruption rate is only ~110 m^3 km^{-2} yr^{-1}, which is similar to that for the St. George Island lavas. Because our data for the Pribilof Islands are still limited, it is not yet clear what such a low rate is due to. It might be due to a separate and unique mantle melting regime beneath these islands, at least compared to the rest of the BSVP where the general increase in eruption rates with decreasing age is observed. While the chance is small, it is also possible that the low eruption rate we have calculated for the Pribilof Islands stems from underestimation of the lava volumes erupted in the region, particularly on and around St. Paul Island. Additional work will be necessary before this issue is completely resolved.

[35] The above calculations show that only ~15% of all the lava in the investigated areas (Imuruk and Teller basalts) was erupted before 3.0 Ma. Some 85% of the lava is younger than 2.5 Ma, and ~30% of it erupted just within the last 500 thousand years. Age information on the submarine volcanism of the Pribilof Ridge are scarce, but if some of these lavas are quite young as might be expected, then the volume of lava erupted within the last 500 thousand years might be even higher than our current estimate of 30%. The increase in eruption rates and lava volumes through time is an interesting observation about the BSVP and suggests either increased local upwelling rates in the mantle leading to severe decompression and associated rapid passive rifting or flexure in the Bering Sea region, close to the North American–Eurasian plate boundary, had major consequences with respect to mantle decompression. In either event, calculated eruption rates do not support the hot spot model for the BSVP magmas in spite of some geochemical similarity to those of ocean island basalts [*Moll-Stalcup*, 1994].

4. Conclusions

[36] New ^{40}Ar/^{39}Ar ages for volcanic rocks from the eastern sector of the Bering Sea Volcanic Province show

Table 3. Change of Height-to-Diameter Ratios of the Volcanic Cones and Their Slope Angles With Time

Time of Eruption, Ma	Height-to-Diameter Ratio	Error, %	Average Slope Angle	Error, °
Modern	0.250	15	40°	1
0.20	0.145	15	38°	3
0.26	0.123	15	36°	3
0.36	0.115	15	35°	3
0.60	0.097	10	33°	3
0.90	0.090	10	30°	2
3.00	0.062	5	28°	2
3.50	0.059	5	27°	1
5.50	0.051	5	25°	1

Table 4. Calculated Eruption Rates for the Studied Part of the Bering Sea Volcanic Province

Volcanic Center	Area, km^2	Volume of Erupted Magma, km^3	Approximate Duration of Volcanic Activity, ka	Eruption Ratio, m^3 km^{-2} yr^{-1}	Estimated Error, %
Imuruk lake volcanic field	1920	110.1	845	68	20
Teller volcanic field	117	2.7	310	75	20
St. George Island	95	11.0	1050	110	10
St. Paul Island	115	6.8	535	111	15
Kookooligit Mountains[a]	830	99.9	980	123	10
SE Nunivak Island	~650	~59	550	165	10
St. Michael volcanic field[b]	~1300	~119	550	166	15

[a]Estimations for Kookooligit Mountains are based on compilation of our data with the data by *Moll-Stalcup* [1994].
[b]Estimates are made only for the western part of the volcanic field.

that eruptions commenced at ~6 Ma and continued intermittently until times too recent to date by this method throughout the whole studied area. The oldest lavas in the province (6–5 Ma) formed with lower eruption rates compared to the lavas erupted later. The early volcanic activity in the Imuruk volcanic field produced some 110 km^3 of lava in an area of ~1920 km^2, which yields an average eruption rate of ~70 m^3 km^{-2} yr^{-1}. A somewhat higher eruption rate (~75 m^3 km^{-2} yr^{-1}) has been computed for the younger (circa 3.5 Ma) basalts of the Teller volcanic field not too far away. Eruption rates increased sharply after ~2.5 Ma, with ~110 m^3 km^{-2} yr^{-1} of basaltic lava forming on St. George Island and up to ~125 m^3 km^{-2} yr^{-1} for younger basalts (~1.2 Ma) in the Kookooligit Mountains (St. Lawrence Island), suggesting either significant changes in stress regime, such as accelerated rifting, or tapping of enriched and possibly hydrous source domains in the upper mantle. The total volume of lava erupted, however, remained modest, with ~11 km^3 erupting on St. George Island in the interval between circa 2.5 Ma and circa 1.5 Ma (these estimates do not include lavas of the Pribilof Ridge where ages of eruptions and duration of volcanic activity are not yet fully characterized), and ~100 km^3 in the Kookooligit Mountains between circa 1.2 Ma and circa 0.3 Ma. Eruptions in the BSVP younger than 0.7 Ma maintained elevated eruption rates, with up to ~165 m^3 km^{-2} yr^{-1} on Nunivak Island and in the St. Michael volcanic field. Combining the new ^{40}Ar/^{39}Ar ages and volume calculations, we estimate that only ~15% of the magma volume in the province erupted by 3.0 Ma. About 30% of all the Cenozoic magmas in the province have erupted just within the last 500 thousand years. Lavas considerably younger than this exist in the province, and though still poorly dated, have been estimated to fall in the 2000–3000 year age range [*Hopkins*, 1963; *Wood and Kienle*, 1990; *Winer et al.*, 2004], suggesting that eruptions are still a possibility in the area. Our follow-up studies are going to focus on dating the youngest lavas using radiocarbon and U series methods for a better understanding of the most recent volcanic activity in the province.

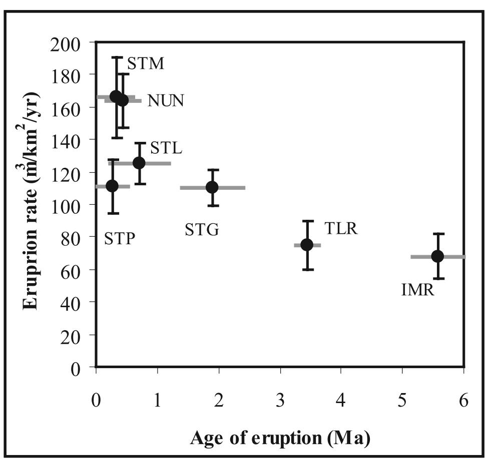

Figure 10. Relations between eruption rate and time of eruption for lavas in the BSVP. The thick gray horizontal lines represent the duration of eruption episodes in individual areas (from Table 1). Error estimates for the eruption rates are calculated on the basis of errors propagated from the estimations of lava areal extents and volumes, as well as the errors for the eruption ages. IMR, Imuruk basalts; KKL, Kookooligit Mountains basalts; NUN, Nunivak Island basalts; STG, St. George Island basanites; STM, St. Michael volcanic field basalts; STP, St. Paul Island basalts; TLR, Teller volcanic field basalts.

[37] **Acknowledgments.** We are grateful to A. Till for her assistance during our preparations for fieldwork. R. Harris, A. Nakak (deceased), and A. Merkulief are thanked for assistance with logistics during fieldwork. M. Johnson is acknowledged for his expert assistance in the Ar geochronology laboratory. V. Akinin is thanked for critically reading an earlier version of this manuscript. Finally, we are indebted to P. Layer and S. Sakimoto for reviewing the manuscript and providing some invaluable comments. This study was supported by NSF grants OPP-9725298 and EAR-0440185 to S.B.M.

References

Amato, J. M., and J. E. Wright (1997), Potassic mafic magmatism in the Kigluaik gneiss dome, northern Alaska: A geochemical study of arc magmatism in an extensional tectonic setting, *J. Geophys. Res.*, *102*, 8065–8084.

Barth, T. W. F. (1956), Geology and petrology of the Pribilof Islands, Alaska, *U.S. Geol. Surv. Bull.*, *1028-F*, 56 pp.

Beget, J., P. Layer, and M. Keskinen (2003), Interactions between volcanism, permafrost, Milankovitch cycles and climate change on the Seward Peninsula, *Geol. Soc. Am. Abstr. Programs*, *35*, 546.

Burch, E. S., and W. Forman (1988), *The Eskimos*, 128 pp., Macdonald Orbis, London.

Comer, C. D., B. M. Herman, and S. A. Zerwick (1987), Geologic report for the St. George Basin planning area, Bering Sea, Alaska, *OCS Rep. MMS 87-0030*, 80 pp., U.S. Dep. of the Inter., Miner. Manage. Serv., Washington, D. C.

Davis, A. S., M. S. Marlow, and F. L. Wong (1994), Petrology of Quaternary basalt from the Bering Sea continental margin, in *Proceedings of the International 1992 Conference on Arctic Margins*, edited by D. K. Thurston and K. Fujita, *MMS Rep. 94-0040*, pp. 124–137, U.S. Miner. Manage. Serv., Anchorage, Alaska.

Dumon, D. E. (1987), *The Eskimos and Aleuts*, 180 pp., Thomas and Hudson, London.
Feeley, T. C., and G. S. Winer (1999), Evidence for fractionation of Quaternary basalts on St. Paul Island, Alaska, with implications for the development of shallow magma chambers beneath Bering Sea volcanoes, *Lithos*, *46*, 661–676.
Fleck, R. J., J. F. Sutter, and D. H. Elliot (1977), Interpretation of discordant ^{40}Ar/^{39}Ar age-spectra of Mesozoic tholeiites from Antarctica, *Geochim. Cosmochim. Acta*, *41*, 15–32.
Frey, H. M., R. A. Lange, and C. M. Hall (2004), Magma eruption rates constrained by ^{40}Ar/^{39}Ar chronology and GIS for the Ceboruco-San Pedro volcanic field, western Mexico, *Geol. Soc. Am. Bull.*, *116*, 259–276.
Godson R. H. (1994), Composite magnetic anomaly map of Alaska and adjacent offshore areas, 1 sheet, scale 1:2,500000, in *The Geology of North America*, vol. G-1, *The Geology of Alaska*, edited by G. Plafker and H. C. Berg , Geol. Soc. of Am., Boulder, Colo.
Hall, C. M., and J. W. Farrell (1995), Laser ^{40}Ar/^{39}Ar ages of tephra from Indian Ocean deep-sea sediments: Tie points for the astronomical and geomagnetic polarity time scales, *Earth Planet. Sci. Lett.*, *133*, 327–338.
Hamilton, T. D. (1994), Late Cenozoic glaciation of Alaska, in *The Geology of North America*, vol. G-1, *The Geology of Alaska*, edited by G. Plafker and H. C. Berg, pp. 813–844, Geol. Soc. of Am., Geol. Soc. of Am., Boulder, Colo.
Hannah, R. S., T. A. Vogel, L. C. Patino, G. E. Alvarado, W. Perez, and D. R. Smith (2002), Origin of silicic volcanic rocks in central Costa Rica: A study of a chemically variable ash-flow sheet in the Tiribi Tuff, *Bull. Volcanol.*, *64*, 117–133.
Hasenaka, T., and I. S. E. Carmichael (1985), The cinder cones of Michoacán-Guanijuato, Central Mexico: Their age, volume and distribution, and magma discharge rate, *J. Volcanol. Geotherm. Res.*, *25*, 105–124.
Hildreth, W., and M. A. Lanphere (1994), Potassium-argon geochronology of a basalt-andesite-dacite arc system: The Mt. Adams volcanic field, Cascade Range of southern Washington, *Geol. Soc. Am. Bull.*, *106*, 1413–1429.
Hoare, J. M., and W. L. Coonrad (1980), The Togiak Basalt, a new formation in southwestern Alaska, *U. S. Geol. Surv. Bull.*, *1482-C*, C1–C11.
Hoare, J. M., W. M. Condon, A. Cox, and G. B. Dalrymple (1968), Geology, paleomagnetism, and potassium-argon ages of basalts from Nunivak Island, Alaska, in *Studies in Volcanology*, edited by R. R. Coats, R. L. Hay, and C. A. Anderson, *Mem. Geol. Soc. Am.*, *116*, 377–413.
Hopkins, D. M. (1963), Geology of the Imuruk Lake area, Seward Peninsula, Alaska, *U.S. Geol. Surv. Bull.*, *1141-C*, 101 pp.
Lipman, P. W. (1995), Declining growth of Mauna Loa during the last 100 000 years: Rates of lava accumulation vs. gravitational subsidence, in *Mauna Loa Revealed: Structure. Composition, History, and Hazards*, *Geophys. Monogr. Ser.*, vol. 92, edited by J. M. Rhodes and J. P. Lockwood, pp. 45–80, AGU, Washington D.C.
Lu, Z., R. Rykhus, T. Masterlak, and K. G. Dean (2004), Mapping recent lava flows at Westdahl Volcano, Alaska, using radar and optical satellite imagery, *Remote Sens. Environ.*, *91*, 345–353.
Marlow, M. S., A. K. Cooper, and M. A. Fisher (1994), Geology of the eastern Bering Sea continental shelf, in *The Geology of North America*, vol. G-1, *The Geology of Alaska*, edited by G. Plafker and H. C. Berg, pp. 271–284, Geol. Soc. of Am., Geol. Soc. of Am., Boulder, Colo.
Menzies, M., and V. R. Murthy (1980), Nd and Sr isotope geochemistry of hydrous mantle nodules and their host alkali basalts: Implications for local heterogeneities in metasomatically veined mantle, *Earth Planet. Sci. Lett.*, *46*, 323–334.
Miller, E. L., and T. L. Hudson (1991), Mid-Cretaceous extensional fragmentation of a Jurassic-Early Cretaceous compressional orogen, Alaska, *Tectonics*, *10*, 781–796.
Moll-Stalcup, E. J. (1994), Latest Cretaceous and Cenozoic magmatism in mainland Alaska, in *The Geology of North America*, vol. G-1, *The Geology of Alaska*, edited by G. Plafker and H. C. Berg, pp. 589–619, Geol. Soc. of Am., Geol. Soc. of Am., Boulder, Colo.
Moll-Stalcup, E. J. (1996), The origin of the Bering Sea Basalt Province, western Alaska, *Geol. Pac. Ocean*, *12*, 671–690.
Nakamura, K., K. H. Jacob, and J. H. Davis (1977), Volcanoes as possible indicators of tectonic stress orientation: Aleutians and Alaska, *Pure Appl. Geophys.*, *115*, 87–112.
Nicolaysen, K., F. A. Frey, K. V. Hodges, D. Wis, and A. Giret (2000), ^{40}Ar/^{39}Ar geochronology of flood basalts from the Kerguelen Archipelago, southern Indian Ocean: Implications for Cenozoic eruption rates of the Kerguelen plume, *Earth Planet. Sci. Lett.*, *174*, 313–328.
Patton, W. W., Jr., and S. E. Box (1989), Tectonic setting of the Yukon-Koyukuk basin and its borderlands, western Alaska, *J. Geophys. Res.*, *94*, 15,807–15,820.
Patton, W. W., Jr., and B. Csejtey Jr. (1971), Preliminary Geologic Investigations of Western St. Lawrence Island, Alaska, *U.S. Geol. Surv. Prof. Pap.*, *684-C*, C1–C15.
Patton, W. W., Jr., and B. Csejtey Jr., (1980), Geologic map of St. Lawrence Island, Alaska, *U.S. Geol. Surv. Misc. Geol. Invest. Ser. Map*, *I-1203*, scale 1:250000.
Patton, W. W., Jr., S. E. Box, and E. J. Moll-Stalcup (1994), Geology of west-central Alaska, in *The Geology of North America*, vol. G-1, *The Geology of Alaska*, edited by G. Plafker and H. C. Berg, pp. 241–269, Geol. Soc. of Am., Geol. Soc. of Am., Boulder, Colo.
Plafker, G., and H. C. Berg (1994), Overview of the geology and tectonic evolution of Alaska, in *The Geology of North America*, vol. G-1, *The Geology of Alaska*, edited by G. Plafker and H. C. Berg, pp. 989–1022, Geol. Soc. of Am., Geol. Soc. of Am., Boulder, Colo.
Renne, P. R., C. C. Swisher, A. L. Deino, D. B. Karner, T. Owens, and D. J. DePaulo (1994), Intercalibration of astronomical and radioisotope time, *Geology*, *22*, 783–786.
Roden, M. F., F. A. Frey, and D. M. Francis (1984), An example of consequent mantle metasomatism in peridotite inclusions from Nunivak Island, Alaska, *J. Petrol.*, *25*, 546–577.
Rowland, S. K., M. E. MacKay, H. Garbeil, and P. J. Mouginis-Mark (1999), Topographic analyses of Kilauea volcano, Hawaii, from interferometric airborne radar, *Bull. Volcanol.*, *61*, 1–14.
Saunders, A. D., and J. Tarney (1984), Geochemical characteristics of basaltic volcanism within backarc basins, in *Marginal Basin Geology* edited by B. P. Kolelaar, and M. F. Howells, pp. 59–76, Oxford Univ. Press, New York.
Stevens, N. F., G. Wadge, and B. Murrey (1999), Lava flow volume and morphology from digitized contour maps: A case study at Mount Etna, Sicily, *Geomorphology*, *28*, 251–261.
Swanson, S. E., D. L. Turner, and R. B. Fores (1981), Petrology and geochemistry of Tertiary and Quaternary basalts from the Seward Peninsula, western Alaska, *Geol Soc Am. Abstr. Programs*, *13*, 563.
Swanson, S. E., M. S. Kay, M. Brearly, and C. M. Scarfe (1987), Arc and back-arc xenoliths in Kurile-Kamchatka and western Alaska, in *Mantle Xenoliths*, edited by P. H. Nixon, pp. 303–318, John Wiley, Hoboken, N. J.
Till, A. B., and J. A. Dumoulin (1994), Geology of Seward Peninsula and Saint Lawrence Island, in *The Geology of North America*, vol. G-1, *The Geology of Alaska*, edited by G. Plafker and H. C. Berg, pp. 141–152, Geol. Soc. of Am., Geol. Soc. of Am., Boulder, Colo.
von Drach, V., B. D. Marsh, and G. J. Wasserburg (1986), Nd and Sr isotopes in the Aleutians: Multicomponent parenthood of island-arc magmas, *Contrib. Mineral. Petrol.*, *92*, 13–34.
West, F. H. (1981), *The Archaeology of Beringia*, 268 pp., Columbia Univ. Press, New York.
Winer, G. S., T. C. Feeley, and M. A. Cosca (2004), Basaltic volcanism in the Bering Sea: Geochronology and volcanic evolution of St. Paul Island, Pribilof Islands, Alaska, *J. Volcanol. Geotherm. Res.*, *134*, 277–301.
Wood, C. A., and J. Kienle (1990), *Volcanoes of North America, United States and Canada*, 354 pp., Cambridge Univ. Press, New York.
York, D. (1969), Least square fitting of a straight line with correlated errors, *Earth Planet. Sci. Lett.*, *5*, 320–324.

A. V. Andronikov, C. M. Hall, and S. B. Mukasa, Department of Geological Sciences, University of Michigan, Ann Arbor, MI 48109, USA. (andron@umich.edu)